Density dependence impacts our understanding of population resilience

Christina M. Hernández^{1,*}
Iain Stott²
David N. Koons³

Roberto Salguero-Gómez¹

- 1. Department of Biology, South Parks Road, Oxford University, Oxford, UK;
- 2. School of Natural Sciences, University of Lincoln, Lincoln, UK;
- 3. Department of Fish, Wildlife, and Conservation Biology, Colorado State University, Fort Collins, Colorado, USA.
- * Corresponding author; e-mail: cmhernan@odu.edu

Manuscript elements: Figure 1, figure 2, figure 3, figure 4, figure 5, figure 6, figure 7, supplemental PDF. All figures are to print in color.

Keywords: COMADRE, COMPADRE, life history strategy, matrix population model, recovery time, transient dynamics.

Manuscript type: Article.

Prepared using the suggested LATEX template for Am. Nat.

Abstract

Current metrics of demographic resilience (e.g., resistance, recovery) summarize how populations respond to the frequent, varied disturbances that ecological systems experience. Much of the application of these metrics has focused on the potential response of populations represented by time-invariant, density-independent structured population models to hypothetical disturbances. Here, we show that density dependence has profound and complex impacts on our understanding of resilience. We examine resilience measures in a flexible structured model with five vital rate parameters (juvenile survival, adult survival, juvenile progression, adult retrogression, and adult reproductive output) with density dependence operating on one vital rate at a time. Depending on which vital rate was subject to density effects, existing measures of demographic resilience (compensation, resistance, and recovery time) either increased or decreased with population density. Moreover, the density-independent model under-predicted the recovery time of the corresponding density-dependent model, with a greater offset for species with longer generation times and higher iteroparity. Our findings demonstrate the importance of underlying non-linear processes when examining demographic resilience, particularly if we hope to predict how natural populations will respond to real disturbances.

Introduction

Ecological systems are exposed to a variety of disturbances. Here, we define disturbance as any a/biotic impact that causes a temporary change in the biological processes that drive population dynamics (sensu Scheffer 2009). Examples of disturbances include a hurricane knocking down adult trees in a stand (Horvitz et al., 1995), pollutants decreasing fertility (Levin et al., 1996), or the introduction of an invader that leads to the decline of endemic species (Doody et al., 2009). As a result of frequent disturbances in natural systems (Turner, 2010), populations may spend little time at equilibrium and instead exhibit 'transient dynamics' (Coulson, 2021; Hastings, 2010; Hastings et al., 2018). Consequently, a major focus of population biology is to understand how populations respond to these myriad disturbances (e.g., Horvitz et al., 1995; McLauchlan et al., 2020; Paniw et al., 2017). As human-induced impacts on biodiversity continue (Butchart et al., 2010; Jaureguiberry et al., 2022) and the frequency of disturbances increases (Turner, 2010), there is an urgent need to identify which species are most likely to persist (Hare et al., 2016; Hernández-Yáñez et al., 2022; Urban, 2015). The study of 'resilience' holds promise for addressing this urgent need (Capdevila et al., 2020; Ingrisch and Bahn, 2018; Scheffer et al., 2015). At its core, resilience is related to concepts of stability: when perturbed, how quickly does the system return to its previous (equilibrium) state (Hastings et al., 2018)?

In natural populations, the demographic resilience framework (Capdevila et al., 2020; Stott et al., 2011) describes how populations are expected to respond to perturbations of population structure. Population structure is the relative distribution of individuals in a population across distinct size, stage, or age classes. Perturbations of population structure might arise from, for example, fires (higher mortality of small than large trees; Sah et al. 2010), hurricanes (more damage to large than small trees; Horvitz et al. 1995), or changes in hunting pressure (cessation of hunting means adults are underrepresented compared to the equilibrium structure; Coulson et al. 2004). This framework of demographic resilience (Capdevila et al., 2020; Stott et al., 2011) is, therefore, inextricably linked to structured population models (*e.g.*, life tables, matrix population models,

integral projection models), where the fates and reproductive contributions of individuals depend on their age, size, and/or developmental stage (Caswell, 2001; Ellner et al., 2016). In these models, the long-term (asymptotic) trajectory of the population is to grow at the rate $r = \log \lambda$ with a stable distribution of individuals across (st)age classes. Transient dynamics arise when the relative size of the (st)age classes changes, potentially causing the short-term growth rate to vary dramatically from λ (Figure 1A; Stott et al. 2011). Natural populations are generally near, but not at, their stable distributions (Williams et al., 2011), leading to mismatches between the expected and realized population growth rate over the short term. An important assumption in this demographic resilience framework is that the vital rates (e.g., survival, maturation, reproduction) that define the matrix population model are density-independent (Stott et al., 2011).

Vital rates are commonly affected by population density, with important implications for population and community dynamics. At the population level, negative density dependence can lead the population size to be stable, to cycle, or to follow chaotic dynamics; the outcome typically depends on the life history of the species (Neubert and Caswell, 2000). In Soay sheep (Ovis aries), interactions between climate and population density cause population size to cycle between increases and crashes (Coulson et al., 2001). In barnacle geese (Branta leucopsis), reproductive output is subject to negative density dependence, causing adult survival to be more important to population dynamics and reproduction less important as population density increases (Layton-Matthews et al., 2019). At low population densities, low encounter rates between individuals can significantly inhibit reproduction, driving small populations to extinction ("Allee effects" Courchamp et al. 1999). Meanwhile, at the community level, density-dependent regulation is crucial to our understanding of species diversity. Theory predicts that coexisting species should exhibit stronger intraspecific competition (i.e., within-population negative density dependence) than interspecific competition (Chesson, 2000). This theoretical expectation is strongly supported by empirical evidence from plant communities, which overwhelmingly exhibit stronger intrathan inter-specific competition (Adler et al., 2018; Metz et al., 2010; Wills et al., 1997).

Matrix population models are generally evaluated at a particular density, rather than being

constructed as explicitly density-dependent models (Crone et al., 2011). For example, when density has been manipulated as part of the experimental design, these models are often constructed as 'high-density' and 'low-density' populations (Meekins and McCarthy, 2002; Oli et al., 2001). While there are examples of explicitly density-dependent matrix population models, (e.g., Bakker et al., 2021; Deangelis et al., 1980; Jensen, 1995; Levin and Goodyear, 1980; Takada and Nakashizuka, 1996), the vast majority of models archived in the COMADRE and COMPADRE databases (Salguero-Gómez et al., 2015; Salguero-Gómez et al., 2016a), a representative sample of published matrix population models, do not explicitly include density effects. Due to limited access to density-dependent models, past work on demographic resilience (Capdevila et al., 2022; Stott et al., 2011; Stott et al., 2012) has not taken density effects into account. Currently, the implicit assumption is that a population's resilience is the same given a certain post-disturbance stage structure, regardless of how the disturbance affects population size. For populations that experience strong density-dependent effects, both the size and structure of the population after a disturbance will have an impact on population dynamics and recovery. For example, the ability of a wild population to resist or recover following a disease outbreak (e.g. Gulland, 1992) could depend on the population size after the disturbance. Likewise, the impact of management actions (e.g., release of wild-reared chicks Kauffman et al. 2004, stage-specific harvesting Fukuda et al. 2021) may differ with population density.

The impact of incorporating density dependence into the analysis of demographic resilience is likely to differ according to life history. For example, a species with low per-capita reproductive output will have little scope for density-dependent effects to further decrease reproductive output. Therefore, negative density dependence on reproductive output may have a limited impact on the demographic resilience of species that invest more in survival than reproduction. Conversely, faster-living species that invest heavily into reproduction may show a strong response of demographic resilience metrics to density-dependent reproduction but a much more limited response to density-dependent survival. So, we may expect that slow-living species will show the greatest impacts on demographic resilience when survival rates are negatively related

to population density, and that fast-living species will show the greatest impacts when reproductive output is negatively related to population density. However, in natural systems these patterns will ultimately depend on the specific density-dependent responses, which are likely to be stage-specific (Gamelon et al., 2024) and to show variation with life history strategy (Bassar et al., 2010). For example, there is evidence that adult survival of a species that invests greatly in vitality might be buffered against the effects of density dependence (Bonenfant et al., 2009) and that growth/maturation is the process most likely to be negatively affected by population density in vertebrates (Bassar et al., 2010).

Here, we explore the implications of negative density dependence on the study of demographic resilience. We take a virtual species approach by simulating negative density-dependent effects on the vital rates of a two-stage matrix population model. The combinations of vital rates in our virtual species are informed by a large database of empirical matrix population models (Salguero-Gómez et al., 2015; Salguero-Gómez et al., 2016a). By varying the combination of vital rate values, we explore a wide range of possible life history strategies. With these models, we ask the following questions: (i) How would the unobserved effects of density change our interpretation of population resilience?, (ii) How do the effects of density on resilience metrics depend on life history strategy? Finally, we investigate the difference in transient behaviour of the density-independent and density-dependent models to (iii) assess whether the density-independent models currently in use could predict qualitative behaviour of the density-dependent models. We conclude by suggesting that the discipline is insufficiently equipped to study demographic resilience in non-linear systems, and offer suggestions to expand our toolbox to examine populations in their natural settings.

Methods

To examine the role of density dependence on demographic resilience across a wide variety of life history strategies, we defined a two-stage population model following Neubert and Caswell (2000). The two stages of this model are non-reproductive and reproductive individuals, with new offspring placed into the non-reproductive class. An important addition here is the potential for individuals to retrogress (*i.e.*, move 'backwards' in their development) from the reproductive class to the non-reproductive class. Including retrogression is important for accurately representing the life cycles of many plants (Salguero-Gómez and Casper, 2010) and some animals (*e.g.*, corals, Cant et al. 2023; marine iguanas, Wikelski and Thom 2000; clown anemonefish Versteeg et al. 2025) that have the ability to drastically decrease in size. For simplicity of language from this point on, we refer to the non-reproductive class as "juveniles" and the reproductive class as "adults." Since some life cycles are best understood in terms of size, here we note that our framework also applies to size-based models, in which case readers might want to think of the classes as "small" and "large" individuals. The transition probabilities that link them would then be growth (instead of progression) and shrinkage (instead of retrogression).

Our population can be projected forward in discrete time (from time t to time t + 1) using the following equation:

$$\begin{bmatrix}
n_j(t+1) \\
n_a(t+1)
\end{bmatrix} = \begin{bmatrix}
\sigma_j * (1-\gamma) & \phi + \sigma_a * \rho \\
\sigma_j * \gamma & \sigma_a * (1-\rho)
\end{bmatrix} \times \begin{bmatrix}
n_j(t) \\
n_a(t)
\end{bmatrix}.$$
(1)

The projection matrix is parameterized with five vital rates: juvenile survival probability (σ_j) , juvenile progression probability (γ) , adult survival probability (σ_a) , adult retrogression probability (ρ) and adult per-capita reproductive output (ϕ) . The population is projected forward in time by multiplying the population vector, composed of the current number of juveniles (n_j) and adults (n_a) , by the projection matrix.

Density dependence in demographic parameters

To explore the effects of density on population resilience, we made each vital rate densitydependent in turn, such that individual performance decreases with increasing density (Bonenfant et al., 2009; Layton-Matthews et al., 2019; Takada and Nakashizuka, 1996). For survival, progression, and reproductive output, we used an exponential form of negative density dependence (Eq. S1). The functional form of density dependence has been a significant area of past research, and is notoriously difficult to identify in empirical systems (Clark et al., 2010; Coulson et al., 2008; Sæther and Engen, 2002). We chose the negative exponential (discrete-time version of the Ricker model Ricker 1954) because it is simple, well-recognized, has a small number of parameters, and because it leads to a stable equilibrium or "carrying capacity" at certain vital rate combinations/ranges for density dependence on juvenile survival, juvenile progression, adult survival, and reproductive output (Neubert and Caswell, 2000). However, we modeled retrogression (ρ) differently. For plants and some animals, the optimal size decreases when resource availability or habitat suitability decreases (Cant et al., 2023; Csergő et al., 2017; Salguero-Gómez and Casper, 2011; Versteeg et al., 2025; Wikelski and Thom, 2000). Since higher density implies lower per-capita resource availability, we would expect the mean size of individuals to decrease with increasing density. Therefore, we used a saturating functional form, where retrogression probability is 0 at low density ($N \approx 0$) and increases asymptotically (Eq. S2). See Supplemental Section S1 for mathematical details.

To compare the response to population density across a wide range of life history strategies, we re-scaled our models. The population densities of, for example, elephants and mice in a given unit of habitat area are on different orders of magnitude (Santini et al., 2018). Rather than being concerned with the absolute population densities, we examined demographic resilience when populations were 'far from carrying capacity' vs. 'near carrying capacity.' So, we scaled our models to a carrying capacity of 1, enabling us to examine the resilience of all life history strategies across the same range of population density values, from N=0 to N=1. We treated all vital rates except reproductive output as free to vary, and then solved for the value of reproductive output (ϕ) that would cause the population to be at a stable equilibrium point at N=1 (see Supplemental Section S2). With this scaling, ϕ is high for life history strategies with low survival (Figure S1). Indeed, to successfully invade, a species with low survival would have

to produce a high number of propagules (Stearns, 1977). Regardless of life history strategy, our scaling for a carrying capacity of 1 means that λ always equals 1 at a density of 1 (Figure S2).

Selecting virtual species

With five vital rates that can vary among species, the possible population models represent a large five-dimensional space. To overcome the challenge of exploring and visualizing results in this high-dimensional space, we selected 16 vital rate combinations to represent the 'space' of life history strategies as archived in the COMADRE (Salguero-Gómez et al., 2016a) and COMPADRE (Salguero-Gómez et al., 2015) databases. In their versions 4.23.3.1 and 6.23.5.0, these databases comprise 3,448 and 8,994 matrix population models for animals and plants, respectively. The majority of these models (>95%) have been digitized from the published literature. Here, we give a brief overview of how we used these databases to select vital rates for our virtual species models. For the full details, see Supplemental Section S3.

We first filtered the COMADRE and COMPADRE databases for high-quality models that represent wild populations under control ("unmanipulated") conditions. Next, we collapsed each of those selected models to the same 2×2 matrix form given in Equation 1 following Salguero-Gómez and Plotkin (2010), using the Rage package (Jones et al., 2022). Finally, we performed a principal component analysis (PCA) on the vital rates calculated from the collapsed matrix models to project them into a reduced dimensional space (Figure 2A). We retained the first two principal component (PC) axes because they captured 70% of the variation among models from COMADRE and COMPADRE (PC1: 43.83%; PC2: 26.25%). PC1 was primarily explained by variation in survival (σ_j , σ_a) and progression (γ), such that longer-lived and late-maturing species score positively on PC1. PC2 was primarily influenced by reproductive output (ϕ), such that species with high reproductive output score positively on PC2 (Supplemental Table S1).

To define our virtual species, we inspected the distribution of empirical values of vital rates in our final set of 1,285 collapsed two-stage models. Based on these distributions, we selected two values for each vital rate (Figure 2A; see Supplemental Section S3). For example, we se-

lected values close to the empirical mean plus/minus one standard deviation for juvenile and adult survival rates. By taking all possible combinations of the vital rates, we generated 16 virtual species. We then projected those virtual species models across density-dependent scenarios (five vital rates by six values of density ranging from 0 to 1) onto the PC axes as defined by the empirical models (Figure 2A). Our virtual species models covered the space of naturally observed populations reasonably well, but we excluded any combinations of virtual species and density dependence scenarios resulting in PC2 scores >5.1 (Figures S3 and S4). This left us with 54 combinations of virtual species and density dependence scenarios (out of 80 total possible combinations).

Density-independent resilience metrics

Demographic resilience measures the *potential response* of a population to a *hypothetical disturbance* to its population structure. There are many different metrics that can be used to measure demographic resilience, and most of them are based on the *transient envelope* (Capdevila et al., 2020; Stott et al., 2011). The transient envelope (blue lines in Figure 1A) comprises the outer boundaries of all possible post-disturbance population trajectories. In other words, a population governed by a given set of time-invariant, density-independent vital rates will always remain within the transient envelope on its way back to its asymptotic behavior (Stott et al., 2011). These transient bounds result from the most extreme initial conditions: the so-called stage-biased trajectories where all individuals are in a single stage class following a disturbance (Townley and Hodgson, 2008).

These trajectories are *relative* to asymptotic dynamics, such that a population starting from its stable stage distribution would maintain a relative population size of 1 over time. For some post-disturbance population structures, the population would change at a rate greater than λ (the boundary that initially shows an increase in relative population size in Figure 1A), while for other initial structures, the population change at a rate less than λ (the boundary that initially shows a decrease in relative population size in Figure 1A).

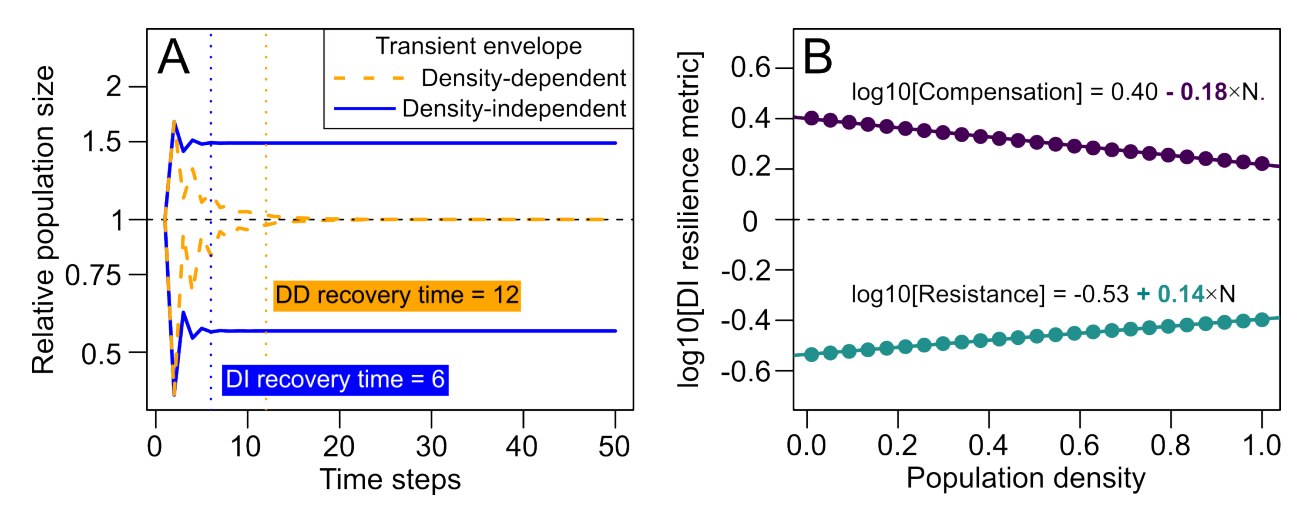


Figure 1: Examples for some key calculations regarding demographic responses to disturbances using transient dynamics. In both examples, the underlying population model exhibits negative density dependence in reproductive output, and the other vital rates are set to the following values: juvenile survival $\sigma_j = 0.4$, juvenile progression $\gamma = 0.9$, adult survival $\sigma_a = 0.6$, and adult retrogression probability $\rho = 0$. (A) Here we show the 'transient envelope' for the density-independent (blue) and density-dependent (orange) models. For this combination of vital rates, the density-independent model requires six time steps to recover back to asymptotic dynamics (blue vertical dotted line). Meanwhile, the density-dependent model requires 12 time steps to recover back to the carrying capacity (orange vertical dotted line). (B) At each value of population density (the plotted points), we calculated the density-independent resilience metrics (compensation in purple, resistance in green) from the density-independent matrix population model evaluated at the corresponding value of population density. We then fit a line to the \log_{10} -transformed resilience metrics, finding in this example that compensation decreased with population density (negative slope), while resistance increased with population density (positive slope). Note that we also calculated the slope of density-independent recovery time in the same way.

Here, we explored how population density, via effects on individual vital rates, would impact previously-studied metrics of demographic resilience (Capdevila et al., 2020; Stott et al., 2011). These previously-studied metrics are density-independent, but we can calculate them for a population projection matrix built at a particular density. In essence, we analyzed how our understanding of resilience would change if demographers had measured vital rates when the population was at low vs. high density. To do so, we calculated *compensation*, *resistance*, and *recovery time* for the (density-independent) population projection matrix built from (density-dependent) vital rates at various values of density between N = 0 and N = 1 (Figure 1B). All density-independent resilience metrics were calculated using the popdemo package in R (Stott et al., 2012).

Compensation. The propensity for a population to 'boom' after a disturbance is referred to as compensation, amplification, or first-time-step reactivity (Capdevila et al., 2020; Capdevila et al., 2022; Stott et al., 2011). Compensation is calculated as the largest possible population size, relative to a population growing at a rate λ , in the first time step after a disturbance (Capdevila et al., 2022). It is the value on the upper branch of the transient envelope one time step after the disturbance. In general, this maximum one-time-step population growth rate would occur if the entire population were concentrated in the most fecund stage class (*e.g.*, the adults in our two-stage model).

Resistance. The ability of a population to prevent further losses after a disturbance is referred to as resistance or first-time-step attenuation. Resistance is calculated as the smallest possible relative population size in the first time step after a disturbance (Capdevila et al., 2024; Stott et al., 2011). In general, this minimum one-time-step population growth rate would be achieved if the entire population were concentrated in the most vulnerable and least fecund stage class (e.g., juveniles in our two-stage model). Populations can vary greatly in their degree of resistance from those whose relative population size changes little following a disturbance (high resistance, metric close to 1) to those whose abundance crashes (low resistance, metric close to 0).

Recovery time. Here, we define recovery time as the number of time steps until all possible post-disturbance initial conditions would converge back to asymptotic dynamics (Stott et al., 2011). Recovery time is calculated by iterating the model from all possible stage-biased (post-disturbance) initial conditions until convergence (blue lines in Figure 1A). A stage-biased initial condition (*i.e.*, following a disturbance) is one where all remaining individuals are in a single stage class. For each possible stage-biased initial condition, we iterated the population model until the one-step-ahead population growth converged to λ using the convt() function in the population package (Stott et al., 2012). We then measured recovery time as the maximum time across the possible initial conditions. In our model, there are two possible stage-biased initial conditions: only adults, and only juveniles. Note that this definition of recovery time is a change from recent publications on demographic resilience which used a definition of recovery time closely based on the damping ratio (*e.g.*, Capdevila et al., 2020; Capdevila et al., 2022). Past analyses have indicated that the damping ratio is a poor measure of time to convergence (Stott et al., 2011).

We analyzed the relationships between vital rates and resilience metrics in our virtual species using linear regression models in R (R Core Team, 2023). For each resilience metric, we fit two separate regression models. First, we fit a linear regression with strictly additive terms for all five vital rates. Second, we fit a linear regression for the first two principal component axes including additive terms and their interaction. We used these models to interpret the importance of different vital rates and the PC axes in driving the values of compensation, resistance, and recovery time by focusing on the effect sizes (*i.e.*, regression coefficients). However, we do not report p-values because they can be substantially affected by design choices in virtual species approaches (White et al., 2014). Specifically, adjusting sample sizes and replication levels across different density dependence scenarios can alter p-values, thereby diminishing their reliability.

We also explored how life history strategy interacted with density-dependent effects on resilience metrics. To do so, we calculated the linear slopes of log_{10} -transformed compensation, resistance, and recovery time with population density (Figure 1B). We calculated these slopes for

each combination of juvenile survival, progression, adult survival, and retrogression across the full range of possible values for those vital rates. To relate these slopes to life history strategy, we focused on how slopes changed with model-specific maximum values of adult survival (σ_a) and progression (γ). We chose these two vital rates because of their clear mathematical connection with generation time (Gaillard et al., 2005), which is itself an important proxy for life history speed (Healy et al., 2019; Paniw et al., 2018; Salguero-Gómez et al., 2016b). When progression rate is high and adult survival is low, species would exhibit precocious maturation and short mature life span, leading to a short generation time—we refer to this type of life history as 'fast.' Conversely, when progression rate is low and adult survival is high, species would have delayed maturation and long mature life span, leading to a long generation time—therefore this would be a 'slow' life history.

Analysis of transient envelopes

The transient dynamics and process of recovery in the density-independent and density-dependent population models we explored here are fundamentally distinct, both biologically and mathematically. Not only did the density-independent metrics of resilience change with population density, but the process of recovery itself differed. Innately, the density-dependent model is attracted back to its equilibrium population size (carrying capacity), while the density-independent model is attracted to the asymptotic growth rate (Figure 1A). Following Stott et al. (2011), we projected our virtual species forward in time from an all-juvenile or all-adult post-disturbance distribution, starting from a population density of 1. Because we tuned our models such that the carrying capacity is at a population size/density of 1, we can compare the transient envelopes from the density-independent and density-dependent cases. For this comparison, the density-independent model uses the vital rates that would be observed at carrying capacity, and then assumes that those vital rates are constant as population density changes during the recovery process. As such, for our virtual species, the density-dependent and density-independent models are the same for the first time step (Figure 1A). However, the entries of the density-dependent

matrix model vary through time as density affects its target parameter: one of the five vital rates in our two-stage matrix population model (Eq. 1). Along the way, these models differ in both population growth/size and population structure, eventually converging to distinct stable population structures.

To compare the density-dependent and density-independent transient periods, we calculated the recovery time in both models. In the density-independent model, the recovery time is (as explained above) the elapsed time before both the upper and lower transient bounds return to following asymptotic dynamics (when solid blue lines becomes flat in Figure 1A; Stott et al. 2012). Because the transient bounds are calculated by iterating the standardized model ($\hat{\bf A} = {\bf A}/\lambda$; Stott et al. 2011), population size in the standardised model stops changing when the model converges (solid blue lines in Figure 1A). In the density-dependent model, the transient bounds will both eventually return to a population size of 1, the carrying capacity we pre-defined for our density-dependent models (dashed orange line in Figure 1A). We defined the density-dependent recovery time as the time until the distance between the upper and lower bound was smaller than 0.1; this distance could be achieved when both bounds cross within 5% of the carrying capacity, or when one of the bounds has reached carrying capacity and the other is 0.1 population size units away. To compare these two values of recovery time, we defined the difference in recovery time ($\Delta RecoveryTime$) as the difference between the density-independent and density-dependent definitions of recovery time.

We also investigated how life history traits relate to the convergence time of the density-dependent model. We focused on generation time as a proxy for the position of the species along the fast-slow continuum (Gaillard et al., 2005), and the degree of parity as a measure of reproductive strategy (Salguero-Gómez et al., 2016b). For generation time, we calculated the average age difference between parents and offspring (Bienvenu and Legendre, 2015). For degree of parity, we calculated evolutionary entropy, which measures how spread out reproduction is across an individual's lifespan (Demetrius, 1977). Previous research has shown that both life history traits adequately capture a species' life history strategy (Healy et al., 2019; Paniw et al.,

2018; Salguero-Gómez et al., 2016b). We calculated both life history traits with the Rage package (Jones et al., 2022).

Results

Density dependence affected our interpretation of demographic resilience. The strength and direction of the impact of density dependence on resilience metrics depended on both life history strategy and the specific vital rate target of density dependence (Figures 2 and 3). Because of our model scaling, faster life histories exhibited stronger density-dependent effects on their overall population growth rate (Figure S4). Indeed, because we scaled the reproductive output (ϕ) so that all virtual species would have a carrying capacity of 1, fast life histories have high reproductive output and high values of population growth rate (λ) at low density (Figure S4).

In our virtual species models, compensation was most strongly influenced by reproductive output (Figure 2B, Supplemental Table S2). Although most vital rates influenced compensation to some extent, the coefficients were both positive and negative (Supplemental Table S2). As a net result, the effect of PC1 on compensation was much smaller than the effect of PC2 (Supplemental Table S2). As such, virtual species with higher reproductive output exhibited higher compensation (Figure 2B). Resistance was most strongly influenced by juvenile survival, with limited influence from other vital rates (Figure 2C; Supplemental Table S2). Recovery time decreased with higher adult survival and juvenile survival, but increased with a higher probability of retrogression (Supplemental Table S2). As a result, recovery time was longest in virtual species corresponding to extreme values of PC1 (both high and low values; Figures 2D and S5C).

Compensation either increased or decreased with higher population density, depending on the vital rate that was affected by density dependence (Figures 3, 4). Compensation always decreased at higher population density (negative slope) when reproductive output was densitydependent, and always increased at higher population density (positive slope) when density dependence acted via juvenile survival (Figure S6). When density dependence operated via adult

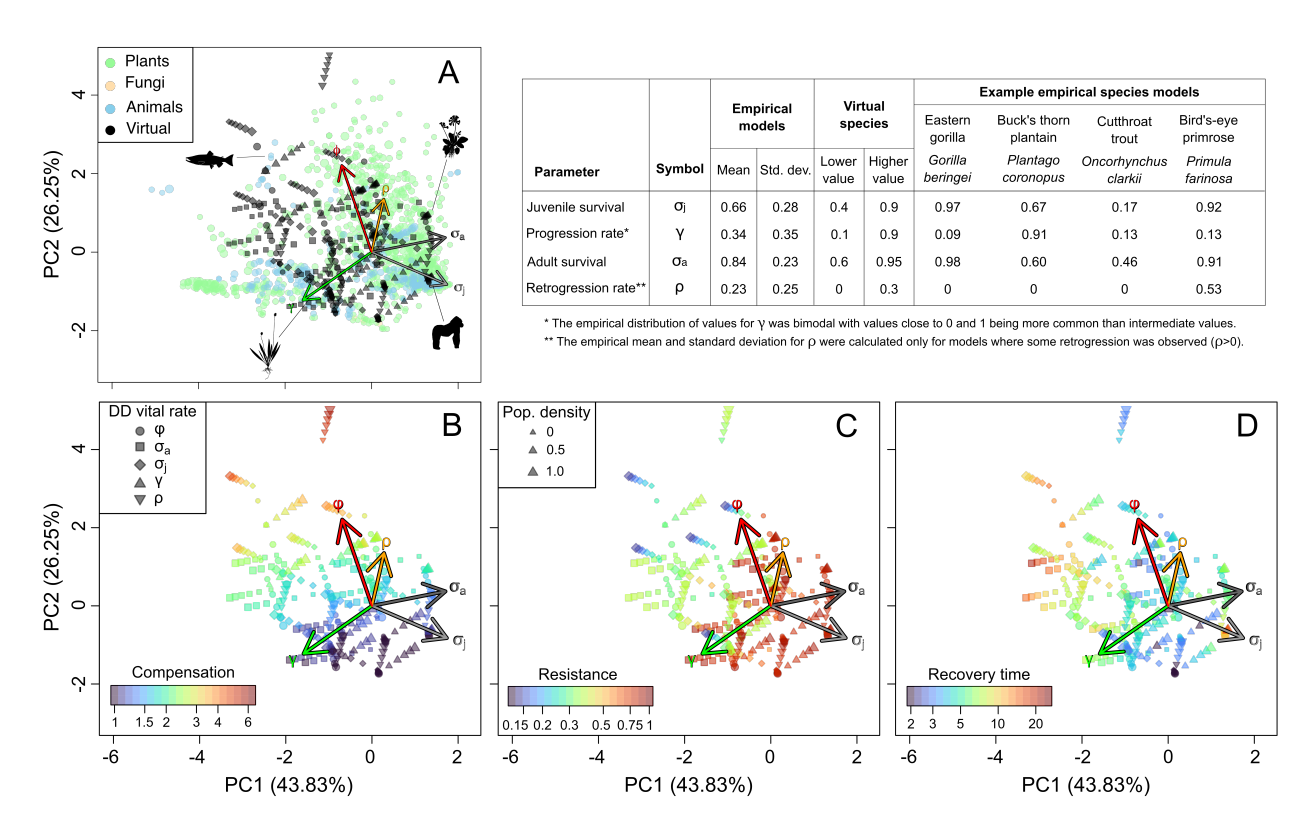


Figure 2: Resilience metrics for our virtual species (A) show strong relationships with demographic rates and axes of life history variation for compensation (B), resistance (C), and density-independent recovery time (D). The PC axes are defined by the empirical models as shown in (A), with the virtual species projected onto the PC axes. The arrows indicate the loading of each vital rate parameter onto the PC axes (Table S1). Life history speed generally increases with PC2 (increasing reproductive output), and decreases with PC1 (increasing survival), such that slow life histories are located towards the bottom-right of the PCA space and fast life histories are located towards the top-left. Each virtual species was modeled with density dependence on each of the five vital rates. For each density-dependent scenario, the virtual species model was calculated for six density values between 0 and 1. In panel A, points are sized according to population growth rate (λ); in panels B-D, symbols are sized according to population density. The example empirical models are indicated by silhouettes (acquired from PhyloPic.org) and are listed in the table based on their clockwise location in the figure, starting from the gorilla.

survival, the response of compensation to density was rather weak (values close to 0, Figures 3, 4B, and S6). For progression and retrogression, compensation tended to increase with density (positive slopes; Figures 3, 4), although the distribution crossed 0 (Figure S6). The response to density was clearly stronger when reproductive output or juvenile survival were density-dependent (Figure 3; absolute value of mean slope \approx 0.2, Supplemental Figure S6), in agreement with our results in Figure 2B that compensation was most closely related to reproductive output and juvenile survival.

In general, fast and slow life histories exhibited similar slopes of compensation across den-

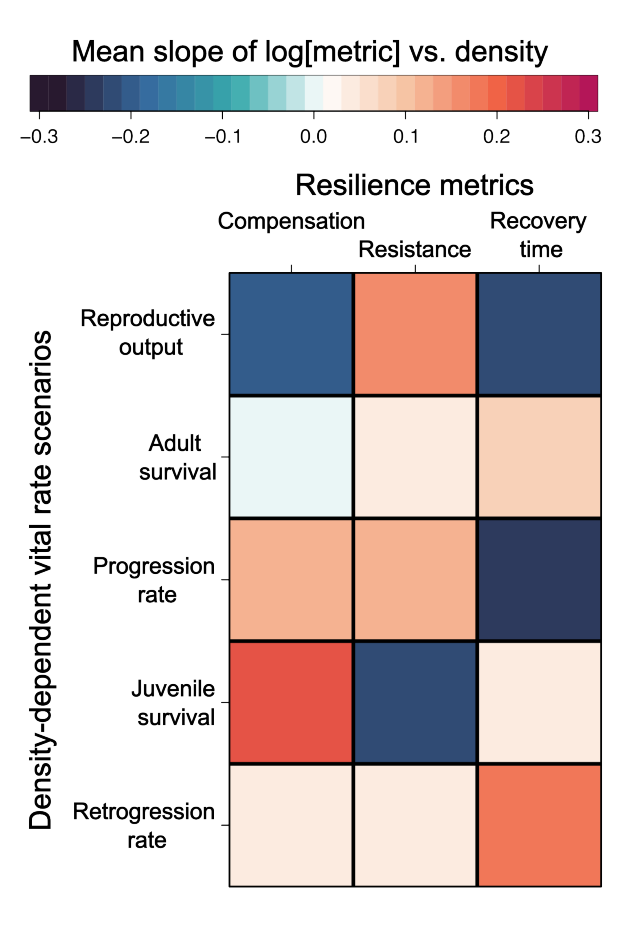


Figure 3: The direction and strength of the change in resilience metrics as density increases depends on which vital rate is the target of density dependence. Here, we summarize the response of resilience metrics (compensation, resistance, and density-independent recovery time) to density dependence on each of the five vital rates (reproductive output, adult survival, progression rate, juvenile survival, and retrogression rate). The colors indicate the mean slope across the full range of tested vital rate combinations.

sities (Figure 4). In other words, moving from a fast to a slow life history did not indicate a change in how strongly compensation would respond to density when reproductive output, progression, and juvenile survival were density-dependent (see how the color contours in Figure 4A,C,D connect the upper left and lower right corners). However, when retrogression was density-dependent, then the strongest response of compensation to population density was in species with a slow life history (delayed progression and high adult survival; Figure 4E).

Resistance tended to increase with population density in all scenarios except for density-dependent juvenile survival (Figures 3, 5, and S12). Like for compensation, the strongest response to population density was observed for the density-dependent reproductive output and

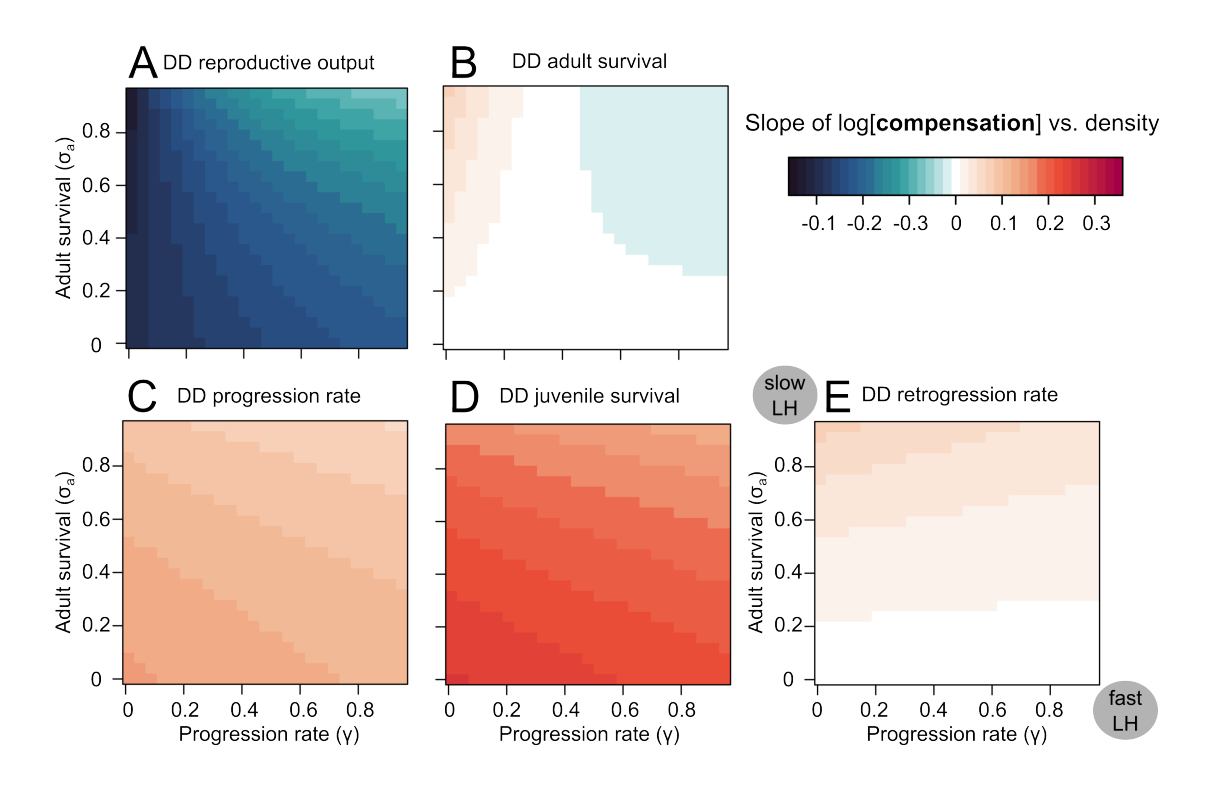


Figure 4: Strength of density effects on compensation varies with both life history strategy and density dependence scenarios. The color contours indicate the slope of compensation as a function of population density. Redder colors indicate that compensation increased with increasing population density, while bluer colors indicate that compensation decreased with increasing population density. Slow life histories are in the upper left of each panel, and fast life histories are in the lower right. These slope surfaces are shown for models with intermediate maximum juvenile survival $\sigma_j = 0.6$ and with maximum retrogression rate $\rho = 0.3$ To see how slope changed across values of maximum juvenile survival and retrogression within each scenario, see figs. S7-S11.

juvenile survival scenarios (Figure 3). When reproductive output was density-dependent, resistance increased with population density most strongly in fast life histories, and the response was weaker in slow life histories (Figure 5A). When juvenile survival was density-dependent, changes in slope were not related to life history speed; instead, the steepest slope emerged when individuals progressed early and had high adult survival (Figure 5D).

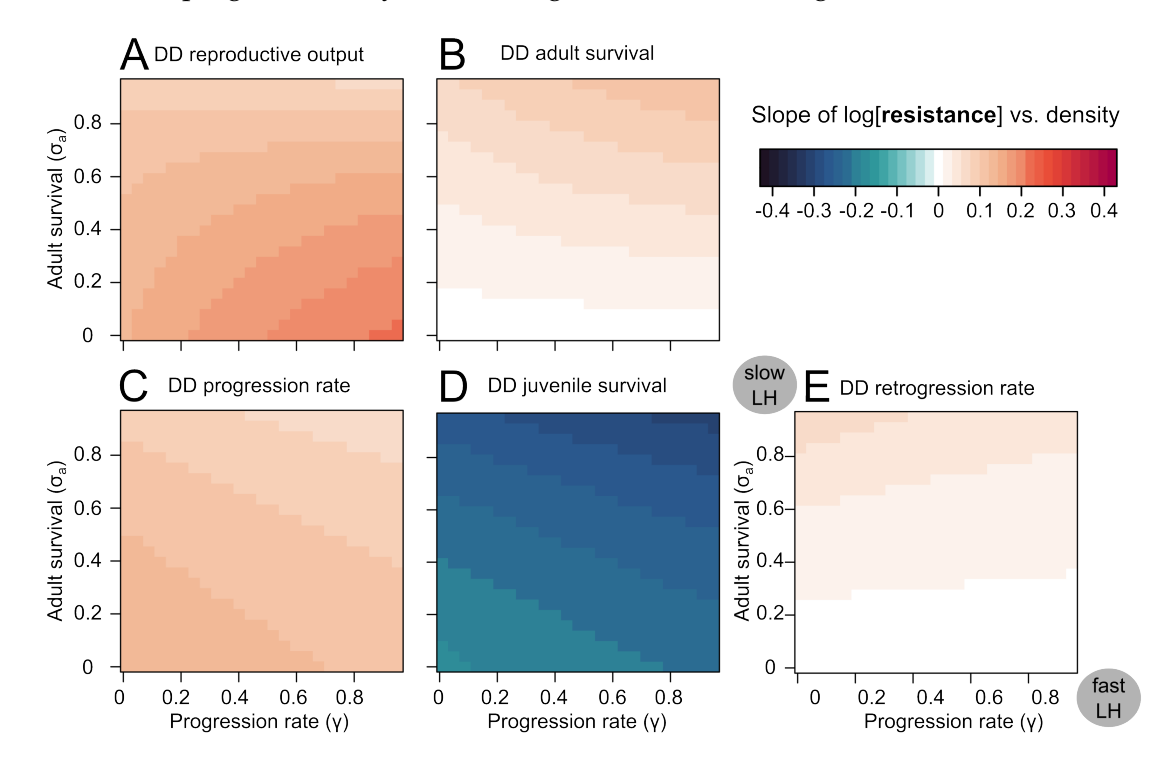


Figure 5: Strength of density effects on resistance varies with both life history speed and density dependence scenarios. The color contours indicate the slope of resistance as a function of population density. Figure details are the same as in Figure 4. To see how slope changed across values of maximum juvenile survival and retrogression within each scenario, see figs. S13-S17.

Responses of recovery time to changes in population density were highly variable across life history and the vital rate target of density dependence (Figures 3, 6). The steepest slopes of recovery time with density were seen when progression, retrogression, or reproductive output were density-dependent (Figure 3). In these scenarios, recovery time decreased at higher population densities for slow life histories, and increased at higher population densities for fast life histories (Figure 6). In the other vital rate scenarios, the response of recovery time to changes in

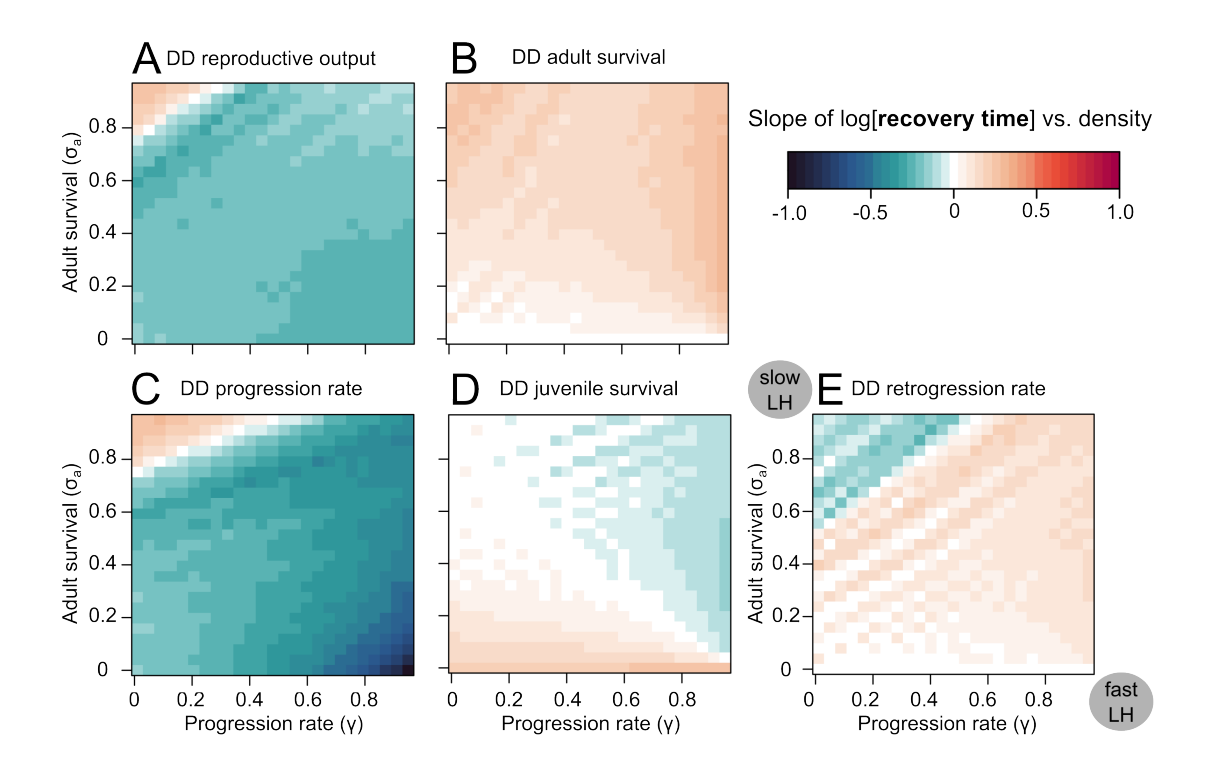


Figure 6: Strength of density effects on density-independent recovery time varies with both life history strategy and density dependence scenarios. The color contours indicate the slope of density-independent recovery time as a function of population density. Figure details are the same as in Figure 4. To see how slope changed across values of maximum juvenile survival and retrogression within each scenario, see figs. S19-S23.

density did not follow any consistent patterns.

Adding density dependence to our demographic models fundamentally changed the process of recovery, as seen in the example transient envelope shown in Figure 1A. The shapes of the transient envelopes varied dramatically across our virtual species and depending on which vital rate is density-dependent (Supplemental Figures S24-S28). The recovery time of the density-independent model nearly always under-predicted the recovery time of the density-dependent model, and the correlation between these measures was very weak (r = 0.03; Figure 7A). We found a fairly strong correlation of $\Delta RecoveryTime$ with both generation time (r = 0.44) and iteroparity (r = 0.37). In other words, as generation time increased or species became more iteroparous, the density-independent model was worse at predicting recovery time of the density-dependent model. If adult survival was density-dependent, then the density-independent model

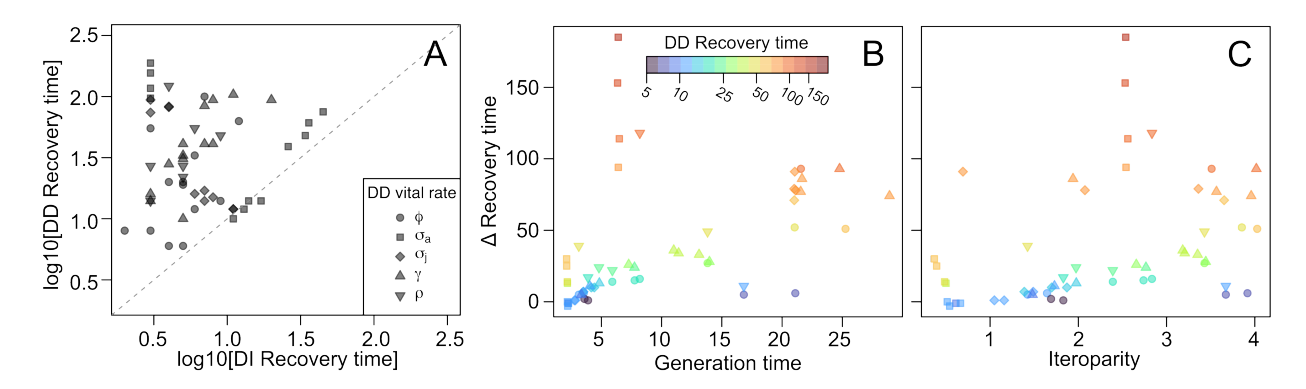


Figure 7: The density-independent (DI) model under-predicts recovery time compared with the density-dependent (DD) model. Panel A shows the relationship between density-independent recovery time and density-dependent recovery time for the virtual species models. $\Delta RecoveryTime$ is positively related to the generation time (B) and degree of iteroparity (C). The different shapes, across all panels, indicate the different density-dependent vital rate scenarios. The color scale shown in panel B applies to panel C as well.

performed particularly poorly (Figure 7B and C).

Discussion

The study of resilience promises to help ecologists and managers understand how populations with diverse life histories may respond to a myriad of disturbances (Enquist et al., 2024). Resilience is closely related to concepts of stability (Hastings et al., 2018) and, in demographic models, long-term asymptotic system behavior (Capdevila et al., 2020; Stott et al., 2011). Although population density has important impacts on individual and population performance (e.g., Bonenfant et al., 2009; Layton-Matthews et al., 2019; Takada and Nakashizuka, 1996), density dependence has been neglected in past studies of demographic resilience. Here, we show that density-dependent vital rates have profound and complex impacts on our understanding of population responses to potential disturbances. Depending on which vital rate (e.g., survival, reproduction) is subject to density effects, existing measures of demographic resilience (compensation, resistance, and recovery time sensu Capdevila et al. 2022; Stott et al. 2011) can either increase or decrease with population density. Importantly, the effects of density dependence on the density-independent resilience metrics was often uncorrelated with life history speed:

the apparent resilience of fast and slow life histories often responded the same way to density dependence. We also found that the recovery time of a density-independent model did not predict the recovery time of the corresponding density-dependent model. In fact, the offset between the density-dependent and density-independent definitions of recovery time were correlated with life history: in species with longer generation time and greater iteroparity, the density-independent model is even worse at predicting recovery time of the underlying density-dependent dynamics.

Our results generally agree with past examinations linking demographic resilience and life history traits. For instance, using 162 populations of 69 animal species from COMADRE and 748 populations of 232 plant species from COMPADRE, Capdevila et al. (2024) showed that species with high reproductive output have greater compensation, weaker resistance and longer recovery time. Here, we found the effects of reproductive output on compensation, resistance, and recovery time to be in the same direction as previously reported. Generation time, a strong marker of life history speed (Gaillard et al., 2005), was found to influence the transient dynamics across 111 mammal species (Gamelon et al., 2014). Likewise, Capdevila et al. (2022) found that slow life histories take longer to recover following a disturbance. Here we similarly report longer recovery times for slow life histories for both density-independent and density-dependent definitions of recovery time), as well as more severe under-estimation of recovery time in the density-independent compared with density-dependent model ($\Delta RecoveryTime$). These authors also found kingdom-specific responses for resistance: resistance increases with generation time in animals but decreases in plants (Capdevila et al., 2024). These kingdom-specific responses may be linked via the more frequent ability of plants to shrink (Salguero-Gómez and Casper, 2010) than in animals (but see Versteeg et al. 2025; Wikelski and Thom 2000), an aspect that can be explicitly explored in future steps via our flexible structured population model. The general agreement between these past studies and our results suggests that density dependence may not be an issue for broad comparative studies of demographic resilience.

For some vital rate targets of density dependence, we found that demographic resilience

increased with population density, despite the density-dependent decrease in individual performance. This counter-intuitive result arises from an indirect effect of density on compensation, via the direct effect of density on population growth rate (λ). Compensation is calculated as the maximum column sum of the standardized population matrix (\hat{A}) . Given that survival rates are bounded between 0 and 1, while fertility rates are often greater than 1 (Salguero-Gómez et al., 2015; Salguero-Gómez et al., 2016a), compensation is often determined by the fertility entries. Therefore, in our two-stage model, compensation is determined by the second column sum of A. So how does the density effect on juvenile survival, which appears only in the first column, impact compensation? The change in compensation arises because of the standardization $(\hat{\bf A} = {\bf A}/\lambda)$. As juvenile survival decreases with density, λ decreases, and so the sum of the second column of $\hat{\mathbf{A}}$ actually increases. The same general principle applies for each of the vital rate scenarios where resistance increased with increasing density. This indirect effect of vital rates on resilience via a change in λ is both striking and easily interpreted in our two-stage model, but we may expect different results in larger, more complex life cycles and their resulting structured population models. For example, if density dependence impacts a stage class that does not control the boom or bust processes (i.e., the most fecund stage and the stage with the lowest survival, respectively), then density dependence would have a limited effect on compensation and resistance, but could still have a meaningful impact on recovery time. Unlike the 2×2 model that we used here in the interest of tractability of incorporating density effects on vital rates, most (93%) matrix population models archived in COMADRE and COMPADRE have more than two stages. In fact, 89% of the models that we used for selecting our virtual species model were 3×3 or larger, and 53% of them were 5×5 or larger (Supplemental Figure S29). Choosing how to parametrize and test the effects of density dependence in these larger models could be quite tricky. For example, in a model where individuals are classified into multiple (>2) size classes, should a negative density-dependent effect on growth affect all size classes equally? This is an ongoing area where more research is needed, to understand the stage-specificity of density-dependent effects (Gamelon et al., 2024).

Our findings have important implications for the study of invasive species. Our results about the relationship between demographic resilience and density dependence suggest an additional mechanism that could help to explain the so-called 'paradox of invasion', wherein locallyadapted species can be replaced by alien species but over time those alien species also become susceptible to invasion by new arrivals (Sax and Brown, 2000). Because populations and communities are experiencing frequent disturbances, the way that a species responds to those disturbances as its density changes may influence its ability to establish and persist. Logically, high compensation at low population density will promote initial establishment, in line with recent evidence that amplification (here referred to as compensation) is a strong predictor of invasiveness (Iles et al., 2016; Jelbert et al., 2019). However, neither of these two works dealt with models that explicitly incorporated density dependence, and our study enables some speculation about how invasiveness may change after initial establishment. For example, a species that exhibits density-dependent reproduction may have a harder time persisting because its compensation in response to disturbances decreases as the population density increases. Conversely, a species that exhibits density dependence on juvenile survival will see even greater compensation in response to disturbances as its population grows and establishes. Therefore, our results suggest that species with high compensation and density-dependent juvenile survival may be more likely to become established and nuisance invaders than species exhibiting density dependence on other vital rates.

Our findings clearly highlight the need for more research aimed at understanding the role of density dependence in populations at risk of extinction. Because resilience metrics change with density in opposite directions depending on the vital rate target, un-modeled density dependence that operates on distinct vital rates for each species could lead to an incorrect ordering of species by their resilience. This would undermine use of the demographic resilience framework to identify and prioritize species for management intervention (Hare et al., 2016; Urban, 2015). Furthermore, we found that density-independent demographic models underestimate recovery time if the underlying vital rates are density-dependent. This underestimation of recovery time

was most severe when species have long generation times and/or high iteroparity. Because animal species with long generation times are also more vulnerable to extinction under climate change (Pearson et al., 2014), these are the same species that are frequently the focus of conservation efforts. In vertebrates, the vital rates with the strongest evidence of density dependence are age or size of maturity (*e.g.* progression in our model) and reproductive output (Bassar et al., 2010). Meanwhile, we found that resilience was most impacted by density-dependent effects when either reproductive output or juvenile survival were the targets of density dependence. Taken together, this suggests that density effects on reproductive output may be the best place to start integrating density dependence into demographic models that are used for management and conservation, as is already standard in fisheries models (Cattoni et al., 2024; Shepherd and Cushing, 1980).

The existing framework of demographic resilience is insufficient to examine the trajectory of a density-dependent model after a disturbance. Demographic resilience measures post-disturbance population growth relative to asymptotic population growth (Stott et al., 2011; Stott et al., 2012), but this standardization makes less sense in density-dependent scenarios where the asymptotic growth rate is zero. Instead, for density-dependent models, measuring relative to carrying capacity would encompass elements of both population size and asymptotic stability. Past work examining the dynamics of density-dependent structured population models has focused on the local stability of the carrying capacity, defining reactivity as the propensity of perturbations from equilibrium to grow before decaying back to the stable equilibrium (Caswell, 2019; Caswell and Neubert, 2005; Neubert and Caswell, 1997). Caswell (Caswell, 2019, p. 207) notes that the local stability approach is based on the inherent system dynamics, while the indices put forward by Stott and colleagues (Capdevila et al., 2020; Stott et al., 2011) are based on the transient responses to a particular initial condition. Here, we focused only on post-disturbance initial conditions where the population is at its carrying capacity, but not at its stable population structure. Further work is needed to analyze transient responses of density-dependent models to perturbations that cause a change in both population density and structure. Still, we have shown that there is

one resilience metric that can be generalized to both density-dependent and density-independent models: recovery time. We found that density-dependent recovery time was longer than density-independent recovery time, indicating that the density-dependent model has a greater probability of long transient periods (Hastings et al., 2018).

Here, we focused on the simplest form of density-dependence: a negative exponential function (Ricker model, Ricker 1954) that applies to a single vital rate at a time, with the same strength in all cases. However, the toolbox of density-dependent approaches is very large. For decades, ecologists and statisticians have argued over which forms of density dependence are most appropriate and when each can be detected or applied (Clark et al., 2010; Coulson et al., 2008; Runge and Johnson, 2002). Beyond the decision of which functional form to apply, there are also decisions about which matrix elements should be affected by density dependence, ranging from all of them (Jensen, 1995) to a critical stage class (Gamelon et al., 2024). The shape and strength of the density-dependent response (*e.g.*, the parameter *b* in Equation S1) is likely to be highly specific to the species, population, and even vital rate (Fukuda et al., 2010). The promise of larger demographic datasets, with collection and analysis made possible by remote sensing and machine learning approaches (Cavender-Bares et al., 2022; Pichler and Hartig, 2023; Sun et al., 2021), is that they may enable a wider estimation of density-dependent processes for population ecology and conservation.

In our modeling framework, density dependence and disturbance are separate processes, but it is likely that they interact in natural systems. In a perennial plant population, the impact of density on both vital rates and population growth rate depended on whether the plot had experienced a fire that year or not (Gornish, 2013). For red deer (*Cervus elaphus*) in Scotland, the cessation of culling led to both changes in population density and population structure, resulting in long-term transient dynamics and density-dependent oscillations (Coulson et al., 2004). Transient life table response experiment (LTRE) analysis holds the potential to disentangle the effects of variation in vital rates and variation in population structure (Knape et al., 2023; Koons et al., 2016), such as could result from the interacting effects of density dependence and disturbance.

However, transient LTREs have so far been underutilized, perhaps because fewer than 40% of the publications archived in the COMADRE and COMPADRE databases (a representative sample of published matrix population models) include data on observed population distributions (Gascoigne et al., 2023).

Conclusion

In spite of the idiosyncratic patterns of resilience across densities and life history strategies, a few patterns with life history strategy remain reliable. Specifically, compensation is greatest and resistance lowest in fast life histories, and vice versa in slow life histories. Additionally, we found that recovery time estimates from the density-independent framework were furthest from the recovery time of the true underlying density-dependent model in virtual species with long generation times and high iteroparity. Therefore, identifying density-dependent effects in more slow-living species, where there are already more conservation concerns (Lande 1998; Purvis et al. 2000, but see Paniw et al. 2018) may be most urgent for predicting responses to disturbance and management intervention. Finally, to truly understand the resilience of natural populations of plants and animals, we must update the demographic resilience framework to accommodate time-varying vital rates. These advances will substantially improve our ability to predict the responses of species to the myriad and increasingly frequent disturbances they face.

Acknowledgments

We thank A. Hector, A. Compagnoni, O. Jones, N. Yoccoz, and three anonymous reviewers for comments on earlier versions of the manuscript. This work was supported by a NERC Pushing the Frontiers grant (NE/X013766/1) to RSG. DNK was supported by US NSF grant DEB-2209765. CMH was additionally supported by a Marie Curie Fellowship [MSCA DensPopDy #10115386] with funding through UKRI [grant number EP/Z002826/1], hosted by RSG.

Statement of Authorship

CMH and RSG conceived of the project. CMH and RSG performed analyses and prepared figures. All authors contributed to interpretation of results. CMH wrote the first draft, and all authors contributed to revising the text.

Data and Code Availability

The data that support the findings of this study are openly available at www.compadre-db.org. All code files required to repeat the analyses are archived at Zenodo [DOI:10.5281/zenodo.13853670].

References

- Adler, P. B., Smull, D., Beard, K. H., Choi, R. T., Furniss, T., Kulmatiski, A., Meiners, J. M., Tredennick, A. T., & Veblen, K. E. (2018). Competition and coexistence in plant communities: Intraspecific competition is stronger than interspecific competition. *Ecology Letters*, 21(9), 1319–1329. https://doi.org/10.1111/ele.13098
- Bakker, V. J., Doak, D. F., & Ferrara, F. J. (2021). Understanding extinction risk and resilience in an extremely small population facing climate and ecosystem change. *Ecosphere*, 12(8), e03724. https://doi.org/https://doi.org/10.1002/ecs2.3724
- Bassar, R. D., López-Sepulcre, A., Walsh, M. R., Turcotte, M. M., Torres-Mejia, M., & Reznick, D. N. (2010). Bridging the gap between ecology and evolution: Integrating density regulation and life-history evolution. *Annals of the New York Academy of Sciences*, 1206(1), 17–34. https://doi.org/10.1111/j.1749-6632.2010.05706.x
- Bienvenu, F., & Legendre, S. (2015). A new approach to the generation time in matrix population models. *American Naturalist*, 185, 834–843. https://doi.org/10.1086/681104

- Bonenfant, C., Gaillard, J.-M., Coulson, T., Festa-Bianchet, M., Loison, A., Garel, M., Loe, L. E., Blanchard, P., Pettorelli, N., Owen-Smith, N., Du Toit, J., & Duncan, P. (2009). Chapter 5 Empirical evidence of density-dependence in populations of large herbivores. In *Advances in Ecological Research* (pp. 313–357, Vol. 41). Elsevier. https://doi.org/10.1016/S0065-2504(09)00405-X
- Butchart, S. H., Walpole, M., Collen, B., Van Strien, A., Scharlemann, J. P., Almond, R. E., Baillie, J. E., Bomhard, B., Brown, C., Bruno, J., et al. (2010). Global biodiversity: Indicators of recent declines. *Science*, 328(5982), 1164–1168. https://doi.org/10.1126/science.1187512
- Cant, J., Reimer, J. D., Sommer, B., Cook, K. M., Kim, S. W., Sims, C. A., Mezaki, T., O'Flaherty, C., Brooks, M., Malcolm, H. A., et al. (2023). Coral assemblages at higher latitudes favor short-term potential over long-term performance. *Ecology*, 104(9), e4138. https://doi.org/10.1002/ecy.4138
- Capdevila, P., Stott, I., Beger, M., & Salguero-Gómez, R. (2020). Towards a comparative framework of demographic resilience. *Trends in Ecology & Evolution*, 35(9), 776–786. https://doi.org/10.1016/j.tree.2020.05.001
- Capdevila, P., Stott, I., Cant, J., Beger, M., Rowlands, G., Grace, M., & Salguero-Gómez, R. (2022). Life history mediates the trade-offs among different components of demographic resilience. *Ecology Letters*. https://doi.org/10.1111/ele.14004
- Capdevila, P., Stott, I., Cant, J., Beger, M., Rowlands, G., Grace, M., & Salguero-Gómez, R. (2024).

 Correction to 'Life history mediates the trade-offs among different components of demographic resilience'. *Ecology Letters*, 27(7), e14468. https://doi.org/https://doi.org/10. 1111/ele.14468
- Caswell, H. (2001). Matrix population models (2nd ed.). Sinauer Associates.
- Caswell, H. (2019). Sensitivity analysis: Matrix methods in demography and ecology. Springer Nature.
- Caswell, H., & Neubert, M. G. (2005). Reactivity and transient dynamics of discrete-time ecological systems. *Journal of Difference Equations and Applications*, 11(4-5), 295–310. https://doi.org/10.1080/10236190412331335382

- Cattoni, V., South, L. F., Warne, D. J., Boettiger, C., Thakran, B., & Holden, M. H. (2024). Revisiting fishery sustainability targets. *Bulletin of Mathematical Biology*, 86(11), 127. https://doi.org/10.1007/s11538-024-01352-7
- Cavender-Bares, J., Schneider, F. D., Santos, M. J., Armstrong, A., Carnaval, A., Dahlin, K. M., Fatoyinbo, L., Hurtt, G. C., Schimel, D., Townsend, P. A., et al. (2022). Integrating remote sensing with ecology and evolution to advance biodiversity conservation. *Nature Ecology & Evolution*, 6(5), 506–519.
- Chesson, P. (2000). Mechanisms of maintenance of species diversity. *Annual review of Ecology and Systematics*, 31(1), 343–366. https://doi.org/10.1146/annurev.ecolsys.31.1.343
- Clark, F., Brook, B. W., Delean, S., Reşit Akçakaya, H., & Bradshaw, C. J. A. (2010). The theta-logistic is unreliable for modelling most census data. *Methods in Ecology and Evolution*, 1(3), 253–262. https://doi.org/10.1111/j.2041-210X.2010.00029.x
- Coulson, T., Ezard, T. H. G., Pelletier, F., Tavecchia, G., Stenseth, N. C., Childs, D. Z., Pilkington, J. G., Pemberton, J. M., Kruuk, L. E. B., Clutton-Brock, T. H., & Crawley, M. J. (2008). Estimating the functional form for the density dependence from life history data. *Ecology*, 89(6), 1661–1674. https://doi.org/10.1890/07-1099.1
- Coulson, T. (2021). We live in a changing world, but that shouldn't mean we abandon the concept of equilibrium. *Ecology Letters*, 24(1), 3–5. https://doi.org/10.1111/ele.13629
- Coulson, T., Catchpole, E. A., Albon, S. D., Morgan, B. J. T., Pemberton, J. M., Clutton-Brock, T. H., Crawley, M. J., & Grenfell, B. T. (2001). Age, sex, density, winter weather, and population crashes in Soay sheep. *Science*, 292(5521), 1528–1531. https://doi.org/10.1126/science. 292.5521.1528
- Coulson, T., Guinness, F., Pemberton, J., & Clutton-Brock, T. (2004). The demographic consequences of releasing a population of red deer from culling. *Ecology*, 85(2), 411–422. https://doi.org/10.1890/03-0009

- Courchamp, F., Clutton-Brock, T., & Grenfell, B. (1999). Inverse density dependence and the Allee effect. *Trends in ecology & evolution*, 14(10), 405–410. https://doi.org/10.1016/S0169-5347(99)01683-3
- Crone, E. E., Menges, E. S., Ellis, M. M., Bell, T., Bierzychudek, P., Ehrlén, J., Kaye, T. N., Knight, T. M., Lesica, P., Morris, W. F., Oostermeijer, G., Quintana-Ascencio, P. F., Stanley, A., Ticktin, T., Valverde, T., & Williams, J. L. (2011). How do plant ecologists use matrix population models? *Ecology Letters*, 14(1), 1–8. https://doi.org/10.1111/j.1461-0248.2010. 01540.x
- Csergő, A. M., Salguero-Gómez, R., Broennimann, O., Coutts, S. R., Guisan, A., Angert, A. L., Welk, E., Stott, I., Enquist, B. J., McGill, B., et al. (2017). Less favourable climates constrain demographic strategies in plants. *Ecology letters*, 20(8), 969–980. https://doi.org/10.1111/ele.12794
- Deangelis, D., Svoboda, L., Christensen, S., & Vaughan, D. (1980). Stability and return times of Leslie matrices with density-dependent survival: Applications to fish populations. *Ecological Modelling*, *8*, 149–163. https://doi.org/10.1016/0304-3800(80)90034-4
- Demetrius, L. (1977). Measures of fitness and demographic stability. *Proceedings of the National Academy of Sciences*, 74, 384–386. https://doi.org/10.1073/pnas.74.1.384
- Doody, J. S., Green, B., Rhind, D., Castellano, C. M., Sims, R., & Robinson, T. (2009). Population-level declines in Australian predators caused by an invasive species. *Animal Conservation*, 12(1), 46–53. https://doi.org/10.1111/j.1469-1795.2008.00219.x
- Ellner, S. P., Childs, D. Z., & Rees, M. (2016). *Data-driven modelling of structured populations: A practical guide to the integral projection model*. Springer International Publishing. https://doi.org/10.1007/978-3-319-28893-2_1
- Enquist, B. J., Erwin, D., Savage, V., & Marquet, P. A. (2024). Scaling approaches and macroecology provide a foundation for assessing ecological resilience in the Anthropocene. *Philosophical Transactions of the Royal Society B: Biological Sciences*, 379(1902), 20230010. https://doi.org/10.1098/rstb.2023.0010

- Fukuda, H., Torisawa, S., Sawada, Y., & Takagi, T. (2010). Ontogenetic changes in schooling behaviour during larval and early juvenile stages of Pacific bluefin tuna *Thunnus orientalis*. *Journal of Fish Biology*, 76(7), 1841–1847. https://doi.org/10.1111/j.1095-8649.2010.02598.x
- Fukuda, Y., Webb, G., Edwards, G., Saalfeld, K., & Whitehead, P. (2021). Harvesting predators: Simulation of population recovery and controlled harvest of saltwater crocodiles /textitCrocodylus porosus. *Wildlife Research*, 48(3), 252. https://doi.org/10.1071/WR20033
- Gaillard, J.-M., Yoccoz, N. G., Lebreton, J.-D., Bonenfant, C., Devillard, S., Loison, A., Pontier, D., & Allaine, D. (2005). Generation time: A reliable metric to measure life-history variation among mammalian populations. *The American Naturalist*, 166(1), 119–123. https://doi.org/10.1086/430330
- Gamelon, M., Araya-Ajoy, Y. G., & Sæther, B.-E. (2024). The concept of critical age group for density dependence: Bridging the gap between demographers, evolutionary biologists and behavioural ecologists. *Philosophical Transactions of the Royal Society B: Biological Sciences*, 379(1916), 20220457. https://doi.org/10.1098/rstb.2022.0457
- Gamelon, M., Gimenez, O., Baubet, E., Coulson, T., Tuljapurkar, S., & Gaillard, J.-M. (2014). Influence of life-history tactics on transient dynamics: A comparative analysis across mammalian populations. *The American Naturalist*, 184(5), 673–683. https://doi.org/10.1086/677929
- Gascoigne, S. J. L., Rolph, S., Sankey, D., Nidadavolu, N., Stell Pičman, A. S., Hernández, C. M., Philpott, M. E. R., Salam, A., Bernard, C., Fenollosa, E., Lee, Y. J., McLean, J., Hetti Achchige Perera, S., Spacey, O. G., Kajin, M., Vinton, A. C., Archer, C. R., Burns, J. H., Buss, D. L., ... Salguero-Gómez, R. (2023). A standard protocol to report discrete stage-structured demographic information. *Methods in Ecology and Evolution*, 14(8), 2065–2083. https://doi.org/10.1111/2041-210X.14164
- Gornish, E. S. (2013). Effects of density and fire on the vital rates and population growth of a perennial goldenaster. *AoB PLANTS*, *5*. https://doi.org/10.1093/aobpla/plt041

- Gulland, F. (1992). The role of nematode parasites in soay sheep (ovis aries l.) mortality during a population crash. *Parasitology*, 105(3), 493–503.
- Hare, J. A., Morrison, W. E., Nelson, M. W., Stachura, M. M., Teeters, E. J., Griffis, R. B., Alexander, M. A., Scott, J. D., Alade, L., Bell, R. J., et al. (2016). A vulnerability assessment of fish and invertebrates to climate change on the northeast US continental shelf. *PloS one*, 11(2), e0146756. https://doi.org/10.1371/journal.pone.0146756
- Hastings, A. (2010). Timescales, dynamics, and ecological understanding. *Ecology*, 91(12), 3471–3480. https://doi.org/10.1890/10-0776.1
- Hastings, A., Abbott, K. C., Cuddington, K., Francis, T., Gellner, G., Lai, Y.-C., Morozov, A., Petrovskii, S., Scranton, K., & Zeeman, M. L. (2018). Transient phenomena in ecology. *Science*, 361(6406), eaat6412. https://doi.org/10.1126/science.aat6412
- Healy, K., Ezard, T. H. G., Jones, O. R., Salguero-Gómez, R., & Buckley, Y. M. (2019). Animal life history is shaped by the pace of life and the distribution of age-specific mortality and reproduction. *Nature Ecology & Evolution*, *3*, 1217–1224. https://doi.org/10.1038/s41559-019-0938-7
- Hernández, C. M., Stott, I., Koons, D. N., & Salguero-Gómez, R. (2025). *Code from: Density dependence impacts our understanding of population resilience. American Naturalist*. Zenodo Digital Repository. https://doi.org/https://zenodo.org/doi/10.5281/zenodo.13853670
- Hernández-Yáñez, H., Kim, S. Y., & Che-Castaldo, J. P. (2022). Demographic and life history traits explain patterns in species vulnerability to extinction. *PloS one*, 17(2), e0263504. https://doi.org/10.1371/journal.pone.0263504
- Horvitz, C. C., McMann, S., & Freedman, A. (1995). Exotics and hurricane damage in three hardwood hammocks in Dade County parks, Florida. *Journal of Coastal Research*, 145–158. https://www.jstor.org/stable/25736005
- Iles, D. T., Salguero-Gómez, R., Adler, P. B., & Koons, D. N. (2016). Linking transient dynamics and life history to biological invasion success. *Journal of Ecology*, 104(2), 399–408. https://doi.org/10.1111/1365-2745.12516

- Ingrisch, J., & Bahn, M. (2018). Towards a comparable quantification of resilience. *Trends in Ecology* & *Evolution*, 33(4), 251–259. https://doi.org/10.1016/j.tree.2018.01.013
- Jaureguiberry, P., Titeux, N., Wiemers, M., Bowler, D. E., Coscieme, L., Golden, A. S., Guerra, C. A., Jacob, U., Takahashi, Y., Settele, J., Díaz, S., Molnár, Z., & Purvis, A. (2022). The direct drivers of recent global anthropogenic biodiversity loss. *Science Advances*, 8(45), eabm9982. https://doi.org/10.1126/sciadv.abm9982
- Jelbert, K., Buss, D., McDonald, J., Townley, S., Franco, M., Stott, I., Jones, O., Salguero-Gómez, R., Buckley, Y., Knight, T., Silk, M., Sargent, F., Rolph, S., Wilson, P., & Hodgson, D. (2019). Demographic amplification is a predictor of invasiveness among plants. *Nature Communications*, 10(1), 5602. https://doi.org/10.1038/s41467-019-13556-w
- Jensen, A. L. (1995). Simple density-dependent matrix model for population projection. *Ecological modelling*, 77(1), 43–48.
- Jones, O. R., Barks, P., Stott, I., James, T. D., Levin, S., Petry, W. K., Capdevila, P., Che-Castaldo, J., Jackson, J., Römer, G., Schuette, C., Thomas, C. C., & Salguero-Gómez, R. (2022). Rcompadre and Rage—two R packages to facilitate the use of the COMPADRE and COMADRE databases and calculation of life-history traits from matrix population models. *Methods in Ecology and Evolution*, 13(4), 770–781. https://doi.org/https://doi.org/10.1111/2041-210X.13792
- Kauffman, M. J., Pollock, J. F., & Walton, B. (2004). Spatial structure, dispersal, and management of a recovering raptor population. *The American Naturalist*, 164(5), 582–597. https://doi.org/https://doi.org/10.1086/424763
- Knape, J., Paquet, M., Arlt, D., Kačergytė, I., & Pärt, T. (2023). Partitioning variance in population growth for models with environmental and demographic stochasticity. *Journal of Animal Ecology*, 92(10), 1979–1991. https://doi.org/10.1111/1365-2656.13990
- Koons, D. N., Iles, D. T., Schaub, M., & Caswell, H. (2016). A life-history perspective on the demographic drivers of structured population dynamics in changing environments. *Ecology Letters*, 19(9), 1023–1031. https://doi.org/10.1111/ele.12628

- Lande, R. (1998). Anthropogenic, ecological and genetic factors in extinction and conservation.

 *Researches on Population Ecology, 40, 259–269. https://doi.org/10.1007/BF02763457
- Layton-Matthews, K., Loonen, M. J. J. E., Hansen, B. B., Coste, C. F. D., Sæther, B.-E., & Grøtan, V. (2019). Density-dependent population dynamics of a high Arctic capital breeder, the barnacle goose. *Journal of Animal Ecology*, 88(8), 1191–1201. https://doi.org/10.1111/1365-2656.13001
- Levin, L., Caswell, H., Bridges, T., DiBacco, C., Cabrera, D., & Plaia, G. (1996). Demographic responses of estuarine polychaetes to pollutants: Life table response experiments. *Ecological Applications*, *6*, 1295–1313. https://doi.org/10.2307/2269608
- Levin, S. A., & Goodyear, C. P. (1980). Analysis of an age-structured fishery model. *Journal of Mathematical Biology*, 9(3), 245–274. https://doi.org/10.1007/BF00276028
- McLauchlan, K. K., Higuera, P. E., Miesel, J., Rogers, B. M., Schweitzer, J., Shuman, J. K., Tepley, A. J., Varner, J. M., Veblen, T. T., Adalsteinsson, S. A., et al. (2020). Fire as a fundamental ecological process: Research advances and frontiers. *Journal of Ecology*, 108(5), 2047–2069. https://doi.org/10.1111/1365-2745.13403
- Meekins, J. F., & McCarthy, B. C. (2002). Effect of population density on the demography of an invasive plant (*Alliaria petiolata*, Brassicaceae) population in a southeastern Ohio forest. *The American midland naturalist*, 147(2), 256–278. https://doi.org/10.1674/0003-0031(2002) 147[0256:EOPDOT]2.0.CO;2
- Metz, M. R., Sousa, W. P., & Valencia, R. (2010). Widespread density-dependent seedling mortality promotes species coexistence in a highly diverse amazonian rain forest. *Ecology*, 91(12), 3675–3685. https://doi.org/10.1890/08-2323.1
- Neubert, M. G., & Caswell, H. (1997). Alternatives to resilience for measuring the responses of ecological systems to perturbations. *Ecology*, 78(3), 653–665. https://doi.org/10.1890/0012-9658(1997)078[0653:ATRFMT]2.0.CO;2

- Neubert, M. G., & Caswell, H. (2000). Density-dependent vital rates and their population dynamic consequences. *Journal of Mathematical Biology*, 41(2), 103–121. https://doi.org/10.1007/s002850070001
- Oli, M. K., Slade, N. A., & Dobson, F. S. (2001). Effect of density reduction on Uinta ground squirrels: Analysis of life table response experiments. *Ecology*, 82, 1921–1929. https://doi.org/10.1890/0012-9658(2001)082\[1921:EODROU\]2.0.CO;2
- Paniw, M., Ozgul, A., & Salguero-Gómez, R. (2018). Interactive life-history traits predict sensitivity of plants and animals to temporal autocorrelation. *Ecology Letters*, 21(2), 275–286. https://doi.org/10.1111/ele.12892
- Paniw, M., Quintana-Ascencio, P. F., Ojeda, F., & Salguero-Gómez, R. (2017). Interacting livestock and fire may both threaten and increase viability of a fire-adapted Mediterranean carnivorous plant. *Journal of Applied Ecology*, 54(6), 1884–1894. https://doi.org/10.1111/1365-2664.12872
- Pearson, R. G., Stanton, J. C., Shoemaker, K. T., Aiello-Lammens, M. E., Ersts, P. J., Horning, N., Fordham, D. A., Raxworthy, C. J., Ryu, H. Y., McNees, J., et al. (2014). Life history and spatial traits predict extinction risk due to climate change. *Nature Climate Change*, 4(3), 217–221. https://doi.org/10.1038/nclimate2113
- Pichler, M., & Hartig, F. (2023). Machine learning and deep learning—a review for ecologists.

 Methods in Ecology and Evolution, 14(4), 994–1016. https://doi.org/https://doi.org/10.

 1111/2041-210X.14061
- Purvis, A., Gittleman, J. L., Cowlishaw, G., & Mace, G. M. (2000). Predicting extinction risk in declining species. *Proceedings of the Royal Society of London. Series B: Biological Sciences*, 267(1456), 1947–1952. https://doi.org/10.1098/rspb.2000.1234
- R Core Team. (2023). R: A language and environment for statistical computing. R Foundation for Statistical Computing. Vienna, Austria. https://www.R-project.org/
- Ricker, W. E. (1954). Stock and recruitment. Journal of the Fisheries Board of Canada, 11(5), 559–623.

- Runge, M. C., & Johnson, F. A. (2002). The importance of functional form in optimal control solutions of problems in population dynamics. *Ecology*, *83*(5), 1357–1371. https://doi.org/10.1890/0012-9658(2002)083[1357:TIOFFI]2.0.CO;2
- Sæther, B.-E., & Engen, S. (2002). Pattern of variation in avian population growth rates. *Philosophical Transactions of the Royal Society of London. Series B: Biological Sciences*, 357(1425), 1185–1195. https://doi.org/10.1098/rstb.2002.1119
- Sah, J. P., Ross, M. S., Snyder, J. R., & Ogurcak, D. E. (2010). Tree mortality following prescribed fire and a storm surge event in slash pine (*Pinus elliottii var. densa*) forests in the Florida Keys, USA. *International Journal of Forestry Research*, 2010(1), 204795. https://doi.org/10.1155/2010/204795
- Salguero-Gómez, R., & Casper, B. B. (2010). Keeping plant shrinkage in the demographic loop. *Journal of Ecology*, 98(2), 312–323. https://doi.org/10.1111/j.1365-2745.2009.01616.x
- Salguero-Gómez, R., & Casper, B. B. (2011). A hydraulic explanation for size-specific plant shrinkage: Developmental hydraulic sectoriality. *New Phytologist*, *189*(1), 229–240. https://doi.org/10.1111/j.1469-8137.2010.03447.x
- Salguero-Gómez, R., Jones, O. R., Archer, C. R., Bein, C., de Buhr, H., Farack, C., Gottschalk, F., Hartmann, A., Henning, A., Hoppe, G., Römer, G., Ruoff, T., Sommer, V., Wille, J., Voigt, J., Zeh, S., Vieregg, D., Buckley, Y. M., Che-Castaldo, J., ... Vaupel, J. W. (2016a).
 COMADRE: A global data base of animal demography. *Journal of Animal Ecology*, 85(2), 371–384. https://doi.org/10.1111/1365-2656.12482
- Salguero-Gómez, R., Jones, O. R., Archer, C. R., Buckley, Y. M., Che-Castaldo, J., Caswell, H., Hodgson, D., Scheuerlein, A., Conde, D. A., Brinks, E., Buhr, H., Farack, C., Gottschalk, F., Hartmann, A., Henning, A., Hoppe, G., Römer, G., Runge, J., Ruoff, T., ... Vaupel, J. W. (2015). The COMPADRE plant matrix database: An open online repository for plant demography. *Journal of Ecology*, 103, 202–218. https://doi.org/10.1111/1365-2745.12334
- Salguero-Gómez, R., Jones, O. R., Jongejans, E., Blomberg, S. P., Hodgson, D. J., Mbeau-Ache, C., Zuidema, P. A., Kroon, H. D., & Buckley, Y. M. (2016b). Fast-slow continuum and

- reproductive strategies structure plant life-history variation worldwide. *Proceedings of the National Academy of Sciences of the United States of America*, 113, 230–235. https://doi.org/10.1073/pnas.1506215112
- Salguero-Gómez, R., & Plotkin, J. B. (2010). Matrix dimensions bias demographic inferences: Implications for comparative plant demography. *The American Naturalist*, 176(6), 710–722. https://doi.org/10.1086/657044
- Santini, L., Isaac, N. J. B., & Ficetola, G. F. (2018). TetraDENSITY: A database of population density estimates in terrestrial vertebrates. *Global Ecology and Biogeography*, 27(7), 787–791. https://doi.org/10.1111/geb.12756
- Sax, D. F., & Brown, J. H. (2000). The paradox of invasion. *Global Ecology and Biogeography*, 9(5), 363–371. https://doi.org/10.1046/j.1365-2699.2000.00217.x
- Scheffer, M. (2009). Critical transitions in nature and society. Princeton University Press.
- Scheffer, M., Carpenter, S. R., Dakos, V., & Van Nes, E. H. (2015). Generic indicators of ecological resilience: Inferring the chance of a critical transition. *Annual Review of Ecology, Evolution, and Systematics*, 46(1), 145–167. https://doi.org/10.1146/annurev-ecolsys-112414-054242
- Shepherd, J. G., & Cushing, D. H. (1980). A mechanism for density-dependent survival of larval fish as the basis of a stock-recruitment relationship. *ICES Journal of Marine Science*, 39(2), 160–167. https://doi.org/10.1093/icesjms/39.2.160
- Stearns, S. C. (1977). The evolution of life history traits: A critique of the theory and a review of the data. *Annual Review of Ecology and Systematics*, 8(1), 145–171. https://doi.org/10.1146/annurev.es.08.110177.001045
- Stott, I., Hodgson, D. J., & Townley, S. (2012). Popdemo: An R package for population demography using projection matrix analysis. *Methods in Ecology and Evolution*, 3(5), 797–802. https://doi.org/10.1111/j.2041-210X.2012.00222.x
- Stott, I., Townley, S., & Hodgson, D. J. (2011). A framework for studying transient dynamics of population projection matrix models. *Ecology Letters*, 14(9), 959–970. https://doi.org/10.1111/j.1461-0248.2011.01659.x

- Sun, Z., Wang, X., Wang, Z., Yang, L., Xie, Y., & Huang, Y. (2021). Uavs as remote sensing platforms in plant ecology: Review of applications and challenges. *Journal of Plant Ecology*, 14(6), 1003–1023.
- Takada, T., & Nakashizuka, T. (1996). Density-dependent demography in a Japanese temperate broad-leaved forest. *Vegetatio*, 124(2), 211–221. https://doi.org/10.1007/BF00045495
- Townley, S., & Hodgson, D. J. (2008). *Erratum et addendum*: Transient amplification and attenuation in stage-structured population dynamics. *Journal of Applied Ecology*, 45(6), 1836–1839. https://doi.org/10.1111/j.1365-2664.2008.01562.x
- Turner, M. G. (2010). Disturbance and landscape dynamics in a changing world. *Ecology*, 91(10), 2833–2849. https://doi.org/10.1890/10-0097.1
- Urban, M. C. (2015). Accelerating extinction risk from climate change. *Science*, 348(6234), 571–573. https://doi.org/10.1126/science.aaa4984
- Versteeg, M. A., MacDonald, C., Bennett-Smith, M. F., Buston, P. M., & Rueger, T. (2025). Individual clown anemonefish shrink to survive heat stress and social conflict. *Science Advances*, 11(21), eadt7079. https://doi.org/10.1126/sciadv.adt7079
- White, J. W., Rassweiler, A., Samhouri, J. F., Stier, A. C., & White, C. (2014). Ecologists should not use statistical significance tests to interpret simulation model results. *Oikos*, 123(4), 385–388. https://doi.org/10.1111/j.1600-0706.2013.01073.x
- Wikelski, M., & Thom, C. (2000). Marine iguanas shrink to survive El Niño. *Nature*, 403(6765), 37–38. https://doi.org/10.1038/47396
- Williams, J. L., Ellis, M. M., Bricker, M. C., Brodie, J. F., & Parsons, E. W. (2011). Distance to stable stage distribution in plant populations and implications for near-term population projections. *Journal of Ecology*, 99(5), 1171–1178. https://doi.org/10.1111/j.1365-2745. 2011.01845.x
- Wills, C., Condit, R., Foster, R. B., & Hubbell, S. P. (1997). Strong density- and diversity-related effects help to maintain tree species diversity in a neotropical forest. *Proceedings of the National Academy of Sciences*, 94(4), 1252–1257. https://doi.org/10.1073/pnas.94.4.1252

References Cited Only in the Online Enhancements.

Janovský, Z., & Herben, T. (2020). Reaching similar goals by different means – differences in life-history strategies of clonal and non-clonal plants. *Perspectives in Plant Ecology, Evolution and Systematics*, 44, 125534. https://doi.org/https://doi.org/10.1016/j.ppees.2020.125534Salguero-Gómez, R. (2018). Implications of clonality for ageing research. *Evolutionary Ecology*, 32, 9–28. https://doi.org/10.1007/s10682-017-9923-2

Online Supplement:

Hernández et al. "Density dependence impacts our understanding of population resilience,"

The American Naturalist

Christina M. Hernández 1,* Iain Stott 2 David Koons 3 Roberto Salguero-Gómez 1

- 1. Department of Biology, University of Oxford, Oxford, UK;
- 2. School of Natural Sciences, University of Lincoln, Lincoln, UK;
- 3. Department of Fish, Wildlife, and Conservation Biology, Colorado State University, Fort Collins, Colorado, USA.
- * Corresponding author; e-mail: cmhernan@odu.edu

S1 Density dependence in demographic parameters

For survival, progression, and reproductive output, we used an exponential form of negative density dependence (Eq. S1). The general form is

$$\alpha(N) = \alpha_{max} e^{-bN},\tag{S1}$$

where α_{max} is the maximum value that a given vital rate can take, and $\alpha(N)$ is that vital rate's value at a given value of population density ($N = n_a + n_j$). For all analyses in this paper, we use b = 1, indicating that all vital rates respond to density-dependence with the same strength.

The only vital rate that did not follow this functional form in our model framework was retrogression (ρ). Instead, we sought a functional form where the probability of retrogression would increase with higher population density. We selected a saturating functional form, where retrogression probability is 0 at very low densities ($N \approx 0$) and increases up to a selected maximum value (asymptotically):

$$\rho(N) = \rho_{max} \ln(N+1) \tag{S2}$$

To ensure that $\rho(1)$ would have a pre-determined value, we set ρ_{max} to $\frac{\rho(1)}{\ln 2}$. This value is the result of re-arranging Equation S1 to solve for ρ_{max} .

S2 Model tuning for density dependence

To compare the response to population density across a wide range of life history strategies, we re-scaled our models to a carrying capacity of 1, enabling us to examine the resilience of all life history strategies across the same range of population density values, from N = 0 to N = 1.

For each density-dependent vital rate scenario, we solved analytically for per-capita reproductive output (ϕ) or maximum per-capita reproductive output (ϕ_{max}) value that corresponds to the population model having its equilibrium population size ('carrying capacity') at a density of 1.

Density is calculated as a simple sum of the number of juveniles and adults ($N(t) = n_j(t) + n_a(t)$). The method for solving for ϕ or ϕ_{max} is as follows:

- 1. Write the population projection matrix with one vital rate as a function of density, following the form $\alpha(N) = \alpha_{max}e^{-bN}$.
- 2. Set this equation to its equilibrium population distribution for juveniles \hat{n}_j and adults \hat{n}_a such that these values are unchanged by projection to the next time step:

$$\hat{\mathbf{n}} = \mathbf{A}(\hat{\mathbf{n}}) \times \hat{\mathbf{n}}.\tag{S3}$$

- 3. Set $\hat{n}_j + \hat{n}_a = 1$.
- 4. Solve the resulting system of equations for ϕ (or ϕ_{max} in the scenario where ϕ is the density-dependent vital rate).

For example, in the case of density-dependent adult survival, we solve the system of equations, given in Eqs. S4 and S5, for ϕ .

$$\begin{bmatrix}
\hat{n}_{j} \\
\hat{n}_{a}
\end{bmatrix} = \begin{bmatrix}
\sigma_{j}(1-\gamma) & \phi + (\sigma_{a,max}e^{-b(\hat{n}_{j}+\hat{n}_{a})})\rho \\
\sigma_{j}\gamma & (\sigma_{a,max}e^{-b(\hat{n}_{j}+\hat{n}_{a})})(1-\rho)
\end{bmatrix} \times \begin{bmatrix}
\hat{n}_{j} \\
\hat{n}_{a}
\end{bmatrix}$$
(S4)

$$\hat{n}_j + \hat{n}_a = 1 \tag{S5}$$

The analytical solutions are as follows:

Density-dependent juvenile survival.

$$\phi = \frac{\left[1 - (1 - \gamma)\sigma_{j,max}e^{-b}\right]\left[(1 - \gamma) - \sigma_a(1 - \rho)(1 - \gamma)\right]}{\gamma(1 - \gamma)\sigma_{j,max}e^{-b}} - \sigma_a\rho \tag{S6}$$

Density-dependent progression.

$$\phi = \frac{-1}{\sigma_i \gamma_{max} e^{-b}} \left[\sigma_a \rho(\sigma_j - 1) + (\sigma_a - 1) \left(1 - \sigma_j (1 - \gamma_{max} e^{-b}) \right) \right]$$
 (S7)

Density-dependent adult survival.

$$\phi = \frac{1 - \sigma_j(1 - \gamma) - \sigma_{a,max}e^{-b} \left[\sigma_j\gamma\rho + (1 - \rho)(1 - \sigma_j(1 - \gamma))\right]}{\sigma_j\gamma}$$
(S8)

Density-dependent retrogression.

$$\phi = \frac{1}{\sigma_j \gamma} \left[(1 - \sigma_a) \left(1 - \sigma_j (1 - \gamma) \right) - \sigma_a \rho_{max} \ln 2(\sigma_j - 1) \right]$$
 (S9)

Density-dependent reproductive output.

$$\phi_{max} = e^b \left(\frac{\left[1 - \sigma_j (1 - \gamma) \right] \left[1 - \sigma_a (1 - \rho) \right]}{\sigma_j \gamma} - \sigma_a \rho \right)$$
 (S10)

S3 Selecting virtual species

We subsetted the COMADRE Animal Matrix Database (Salguero-Gómez et al., 2016) and the COMPADRE Plant Matrix Database (Salguero-Gómez et al., 2015) to matrix population models that are ergodic, irreducible, and primitive. Doing so guarantees the existence of a single dominant eigenvalue (Caswell, 2001, pp. 83-85). We imposed a series of selection criteria on the 3,488 matrix population models available in COMADRE (v. 4.23.3.1) and 8,994 models in COMPADRE (v. 6.23.5.0) to ensure fair comparisons. The criteria are as follows: We retained only models (1) built from demographic data on *both* survival and reproduction, so complete life-cycle information was available; (2) collected in observational ("wild", *i.e.*, non-laboratory) settings without experimental manipulations so the models would reflect the dynamics of natural populations; and (3) published and digitized such that survival and reproduction are separable (*i.e.*, there are

separate **F** and **U** matrices). The latter criterion is particularly necessary here to separate the proportion of the matrix element $a_{1,2}$ that corresponds to reproductive output vs. to (potentially) retrogression. Finally, (5) we excluded models with clonal reproduction because permitting fair comparisons between studies with and without clonal reproduction requires careful consideration of ramet vs. genet dynamics (Janovský and Herben, 2020) and their emergent vital rates (Salguero-Gómez, 2018). As such, in our virtual species model, we also do not include clonal reproduction.

For each matrix population model that met our criteria, we coerced it into the same two-stage model that we are using (see Equation 1 in the main text), that is, a two stage model. When models are digitized for the databases, each stage of the model is identified as a propagule, an active member of the population, or a dormant member of the population. Based on the non-zero columns of the fertility (\mathbf{F}) matrix, we can also identify each life stage as reproductive or non-reproductive. With the columns of the fertility (\mathbf{F}) and survival-growth (\mathbf{U}) matrices correctly identified, we can collapse the models down into a 2 × 2 matrix model (Salguero-Gómez and Plotkin, 2010). This last step was performed using the $mpm_collapse$ function in the Rage package (Jones et al., 2022) in the R programming language.

We then eliminated any collapsed models with incorrect survival values (σ_j or $\sigma_a > 1$). Finally, we restricted our set of observed models to those with a population growth rate (λ , the dominant eigenvalue of the projection matrix) between 1.0 and 1.6. We chose this range as a realistic comparison with our density-dependent models: at equilibrium ("carrying capacity"), our virtual species models will have $\lambda = 1$ and in early tests of the density-dependent reproductive output scenario, the highest population growth (at $N \to 0$) was $\lambda \approx 1.6$. Finally, we removed models with extremely high or extremely low reproductive output, with outliers defined as values for ϕ that fall outside of the interval [LQ - 1.5 * IQR, UQ + 1.5 * IQR], where LQ is the lower quartile, UQ is the upper quartile, and IQR is the interquartile range. This final step resulted in a matrix population model for 410 animal, 872 plant, and three fungi populations, representing 100, 204, and one species, respectively (Supplemental Materials Table S4).

Supplemental References

- Caswell, H. (2001). Matrix population models (2nd ed.). Sinauer Associates.
- Janovský, Z., & Herben, T. (2020). Reaching similar goals by different means differences in life-history strategies of clonal and non-clonal plants. *Perspectives in Plant Ecology, Evolution and Systematics*, 44, 125534. https://doi.org/https://doi.org/10.1016/j.ppees.2020.125534
- Jones, O. R., Barks, P., Stott, I., James, T. D., Levin, S., Petry, W. K., Capdevila, P., Che-Castaldo, J., Jackson, J., Römer, G., Schuette, C., Thomas, C. C., & Salguero-Gómez, R. (2022). Rcompadre and Rage—two R packages to facilitate the use of the COMPADRE and COMADRE databases and calculation of life-history traits from matrix population models. *Methods in Ecology and Evolution*, 13(4), 770–781. https://doi.org/https://doi.org/10.1111/2041-210X.13792
- Salguero-Gómez, R. (2018). Implications of clonality for ageing research. *Evolutionary Ecology*, 32, 9–28. https://doi.org/10.1007/s10682-017-9923-2
- Salguero-Gómez, R., Jones, O. R., Archer, C. R., Bein, C., de Buhr, H., Farack, C., Gottschalk, F., Hartmann, A., Henning, A., Hoppe, G., Römer, G., Ruoff, T., Sommer, V., Wille, J., Voigt, J., Zeh, S., Vieregg, D., Buckley, Y. M., Che-Castaldo, J., ... Vaupel, J. W. (2016). COMADRE: A global data base of animal demography. *Journal of Animal Ecology*, 85(2), 371–384. https://doi.org/10.1111/1365-2656.12482
- Salguero-Gómez, R., Jones, O. R., Archer, C. R., Buckley, Y. M., Che-Castaldo, J., Caswell, H., Hodgson, D., Scheuerlein, A., Conde, D. A., Brinks, E., Buhr, H., Farack, C., Gottschalk, F., Hartmann, A., Henning, A., Hoppe, G., Römer, G., Runge, J., Ruoff, T., ... Vaupel, J. W. (2015). The COMPADRE plant matrix database: An open online repository for plant demography. *Journal of Ecology*, 103, 202–218. https://doi.org/10.1111/1365-2745.12334
- Salguero-Gómez, R., & Plotkin, J. B. (2010). Matrix dimensions bias demographic inferences: Implications for comparative plant demography. *The American Naturalist*, 176(6), 710–722. https://doi.org/10.1086/657044

S4 Supplemental Figures and Tables

Table S1: The contribution of each vital rate to the first two principal component axes (PC1 and PC2). Loadings in bold indicate a high contribution (greater than ± 0.50) of the life-history trait to the PC axis.

Vital rate	Symbol	PC1	PC2
Juvenile survival	σ_i	0.579	0.269
Progression	γ	-0.529	-0.408
Adult survival	σ_a	0.569	0.123
Retrogression	ρ	0.094	0.450
Reproductive output	φ	-0.230	0.735
Proportion of variance		0.438	0.263
Cumulative proportion of variance		0.438	0.701

Table S2: The effects of vital rates and principal component axes on the resilience metrics of compensation, resistance, and recovery time in our virtual species. For each resilience metric, we fit two separate regression models. First, we fit a linear regression with strictly additive terms for each vital rate. Second, we fit a linear regression for the principal component axes including additive terms and their interaction.

Vital rate	Symbol	Regression coefficient		
		Compensation	Resistance	Recovery Time
Juvenile survival	σ_{j}	-0.402	0.838	-3.679
Progression	$\dot{\gamma}$	-0.351	-0.085	0.588
Adult survival	σ_a	0.626	-0.076	-4.689
Retrogression	ρ	0.152	0.048	2.687
Reproductive output	ϕ	0.771	-0.036	0.201
PC axis 1		-0.094	0.135	-0.805
PC axis 2		0.604	-0.060	-0.383
Interaction PC1 and P	C2	-0.023	0.002	-0.705

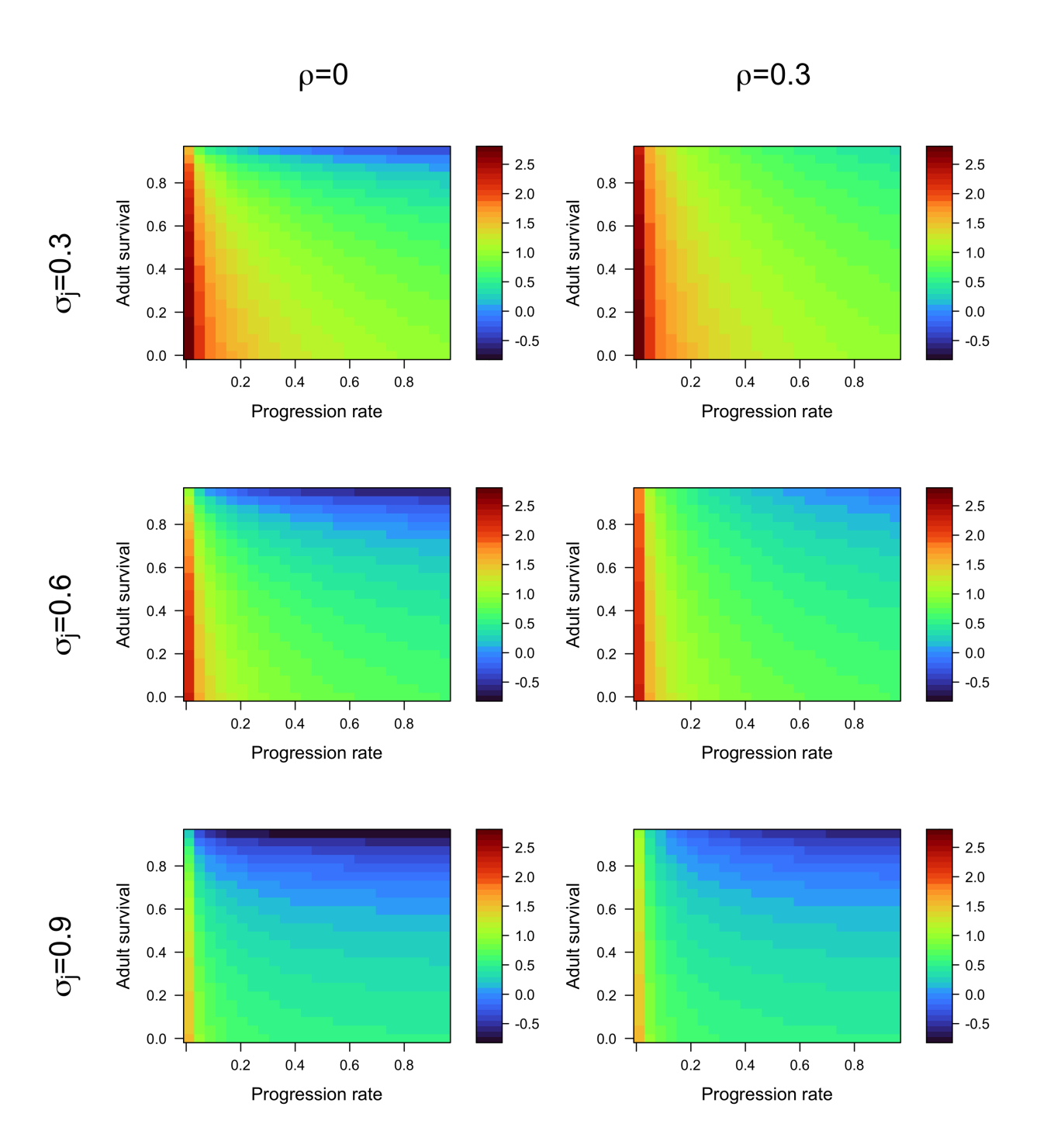


Figure S1: An example of how our model scaling affects maximum reproductive output (ϕ_{max}) across other vital rates. In this case, reproductive output is density-dependent, and the model is scaled such that the population is at its carrying capacity ($\lambda = 1$) when population density ($n_a + n_j$) is equal to 1. In each panel, we show how ϕ_{max} varies across progression (γ) and adult survival (σ_a) for a given value of juvenile survival (σ_b) and retrogression (γ). The color scales are $\log_{10}(\phi_{max})$.

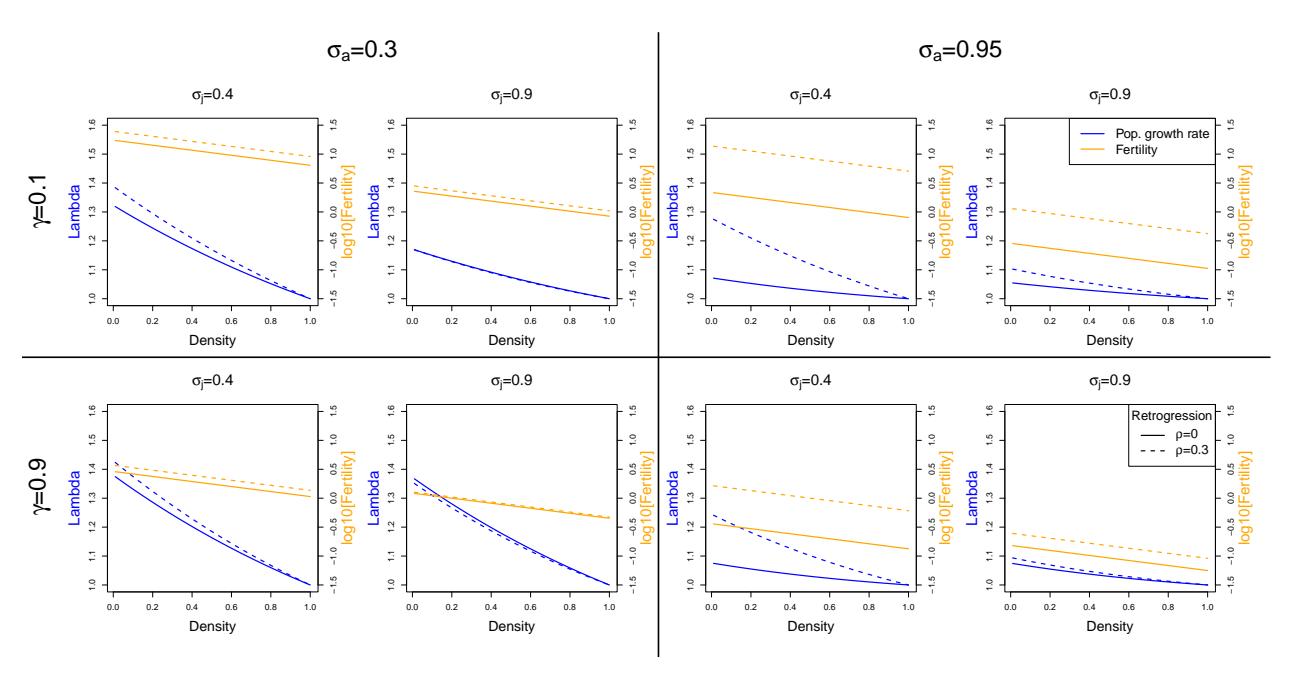


Figure S2: Population growth rate (λ) and per-capita reproductive output (ϕ) across population density for 16 virtual species models, density dependence impacts the per-capita reproductive output (ϕ).

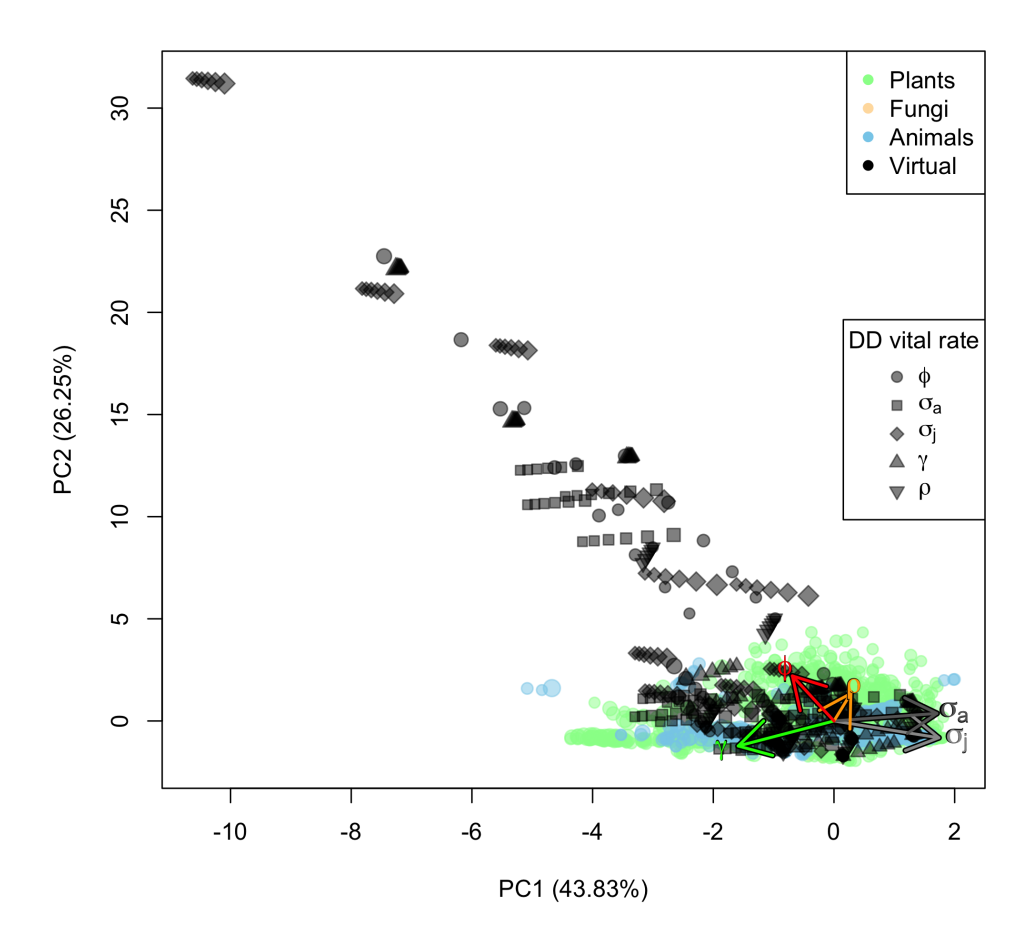


Figure S3: Some of the virtual species and density-dependent vital rate scenarios corresponded to extreme values of PC2, falling far from the space defined by empirical models. he parameters are: juvenile survival (σ_j) , juvenile progression (γ) , adult survival (σ_a) , adult retrogression (ρ) , and reproductive output (ϕ) . The PCA space is defined by the observed models (colored circles, sized according to their asymptotic population growth rate, λ). The virtual species, shown in black, were then projected onto the PCA space. Each virtual species was modelled with density dependence on each of the five vital rates (shown with different shapes), and each density-dependent scenario was plotted for six values of density between 0 and 1, sized according to λ .

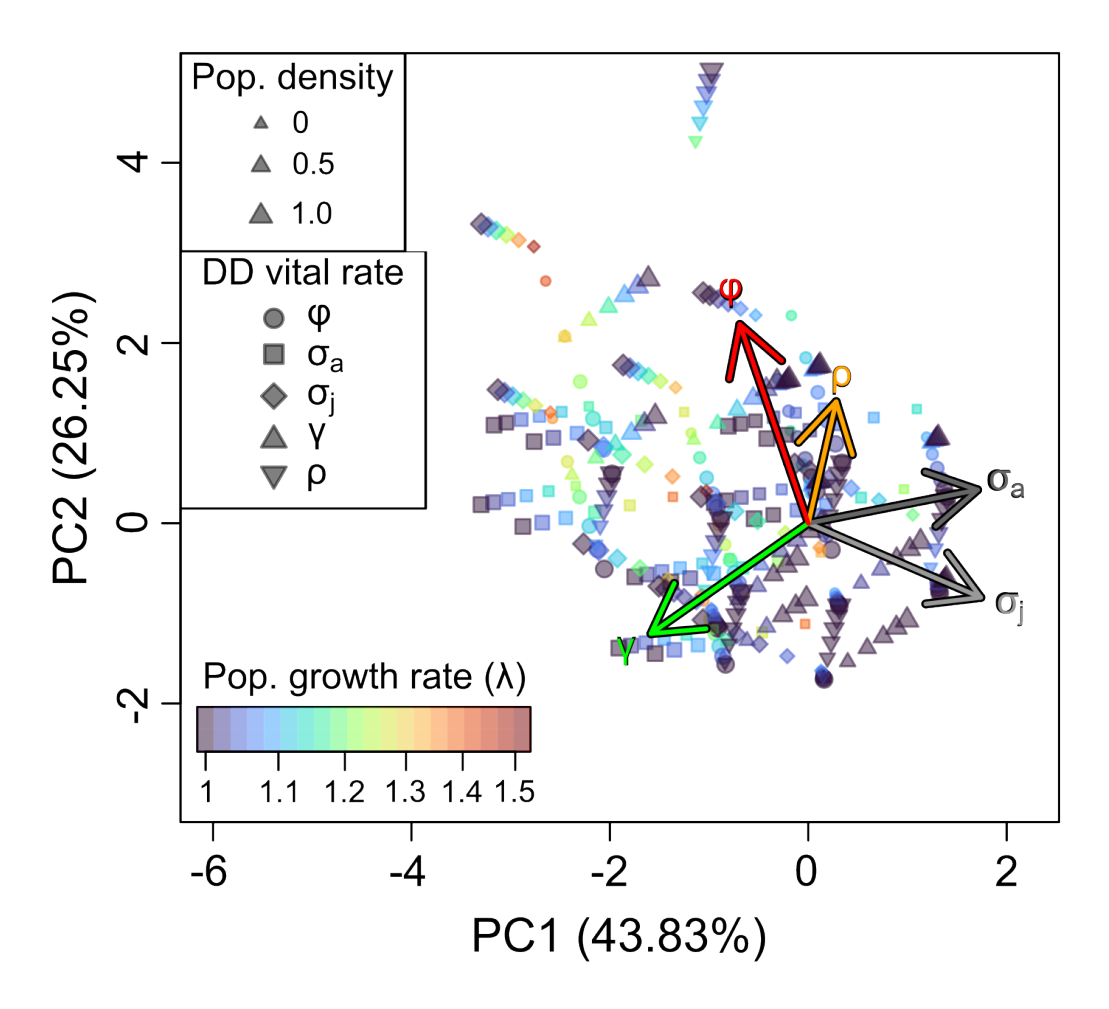


Figure S4: Population growth rate in virtual species models changes across life history strategies and density-dependent scenarios. The vital rates are: juvenile survival (σ_j) , adult survival (σ_a) , juvenile progression (γ) , adult retrogression (ρ) , and reproductive output (ϕ) . The principal component (PC) axes were defined using empirical models of 1,285 natural/wild populations of animals and plants (see Fig. S3). The virtual species have then been projected onto the PC axes. Each virtual species was modeled with density dependence on each of the five vital rates. For each density-dependent scenario, the virtual species model was calculated for six values of density between 0 and 1 (plot symbols sized according to population density).

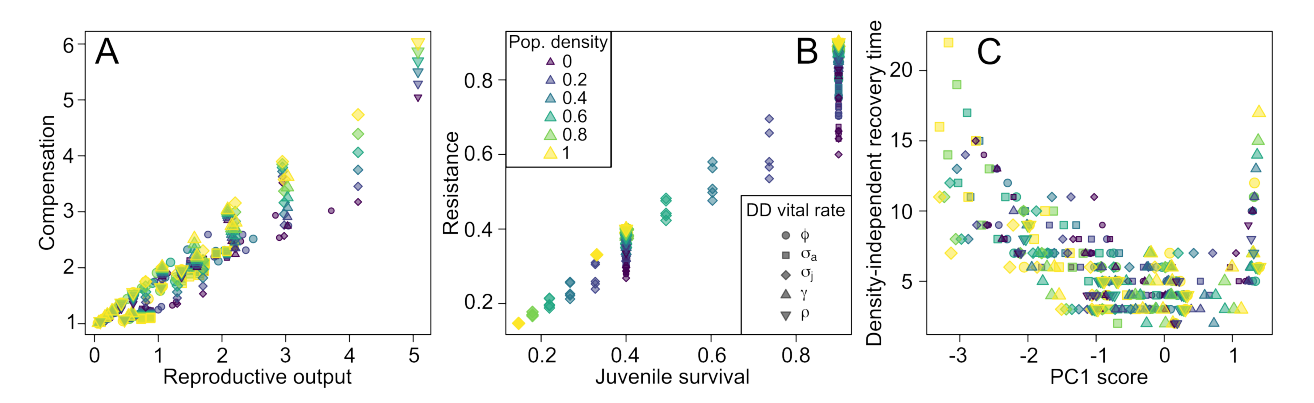


Figure S5: Resilience metrics for our virtual species show strong relationships with demographic rates. The demographic rates with the strongest relationships to the resilience metrics were (A) reproductive output for compensation and (B) juvenile survival for resistance. Density-independent recovery time showed a complicated and non-linear relationship with demographic rates, and density-independent recovery times were longest for virtual species with extreme scores on PC1.

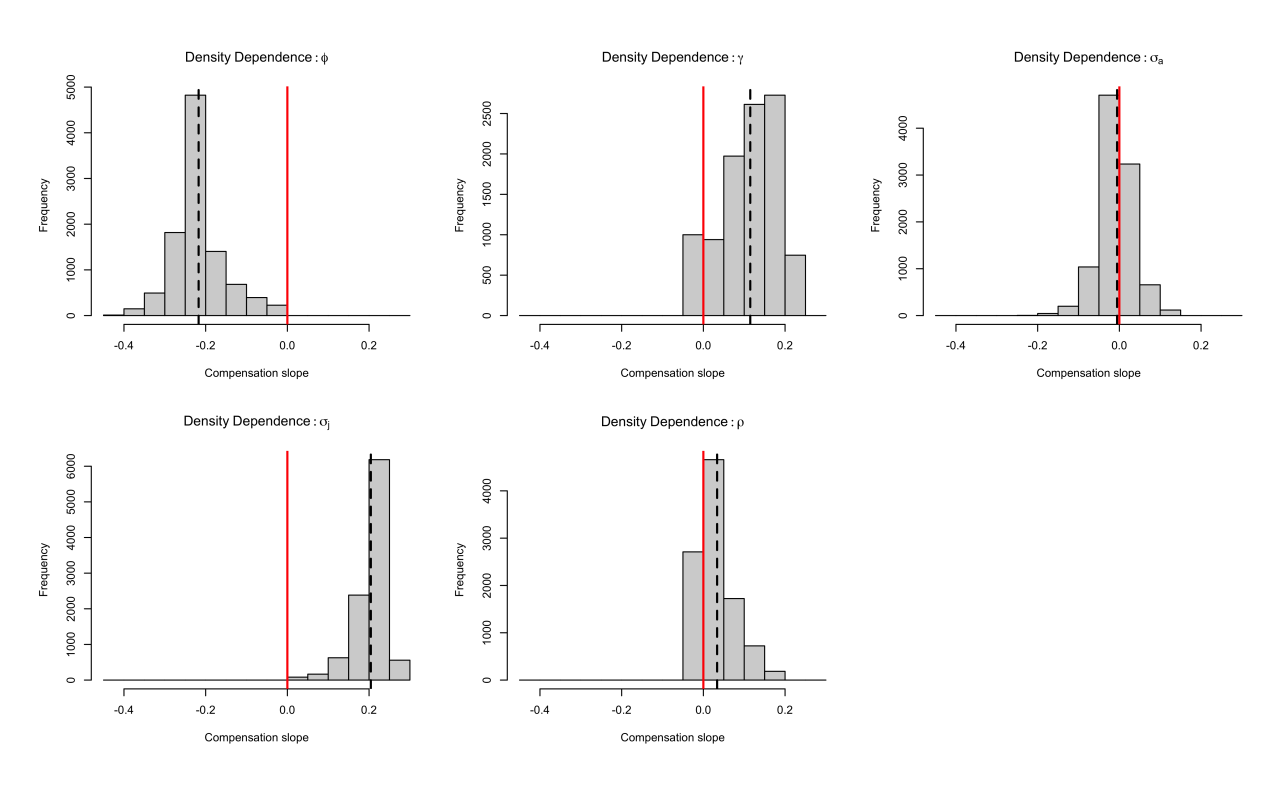


Figure S6: The distribution of compensation slope values depends on which vital rate is the target of density dependence. For each density dependence scenario, we calculated the slope of compensation across densities (*i.e.*, a in $\log_{10}(C) = a * N + b$, where N is population density and C is the compensation of the population projection matrix calculated at each value of N) for the full range of possible vital rates: $\sigma_j \in [0.01, 1]$; $\gamma \in [0.01, 0.95]$; $\sigma_a \in [0, 0.95]$; and $\rho \in [0, 1]$. For each vital rate, we calculated slopes at 10 values, yielding a total of 10^4 vital rate combinations for each density dependence scenario. In each panel, a slope of 0 is highlighted with a solid red line, and the mean value of slopes across all tested vital rate combinations is shown with a thick vertical dashed line.

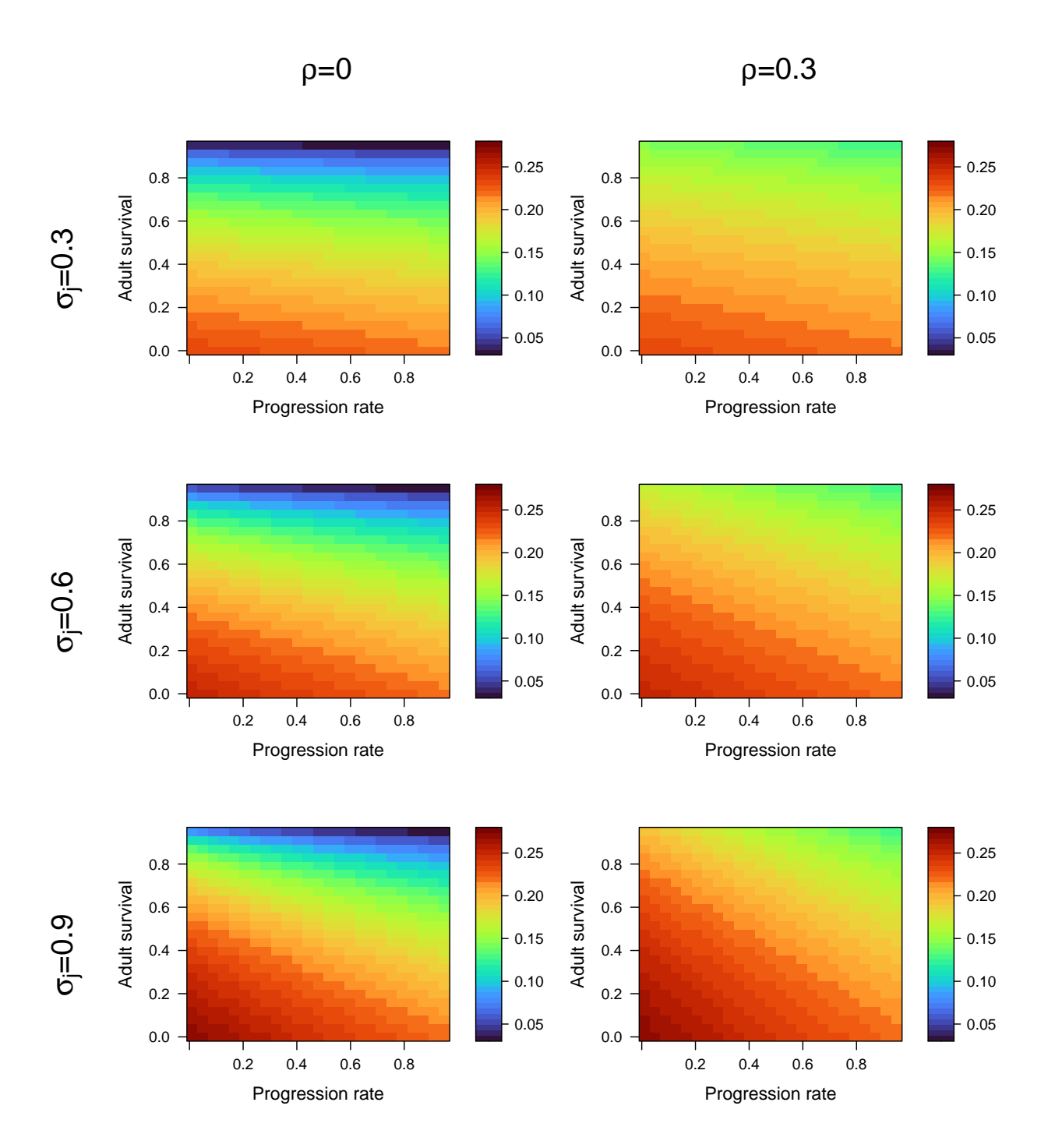


Figure S7: Strength of density effects on compensation when juvenile survival is density-dependent. We calculated the slope of compensation across population densities (log $C \sim N_t$) for many possible parameter combinations across: $\sigma_a \in [0,0.95]$, $\gamma \in [0.01,0.95]$, $\sigma_j = 0.3,0.6,0.9$, and $\rho = 0,0.3$. A single color scale is used for all panels. Slow life histories are in the upper left of each panel, and fast life histories are in the lower right.

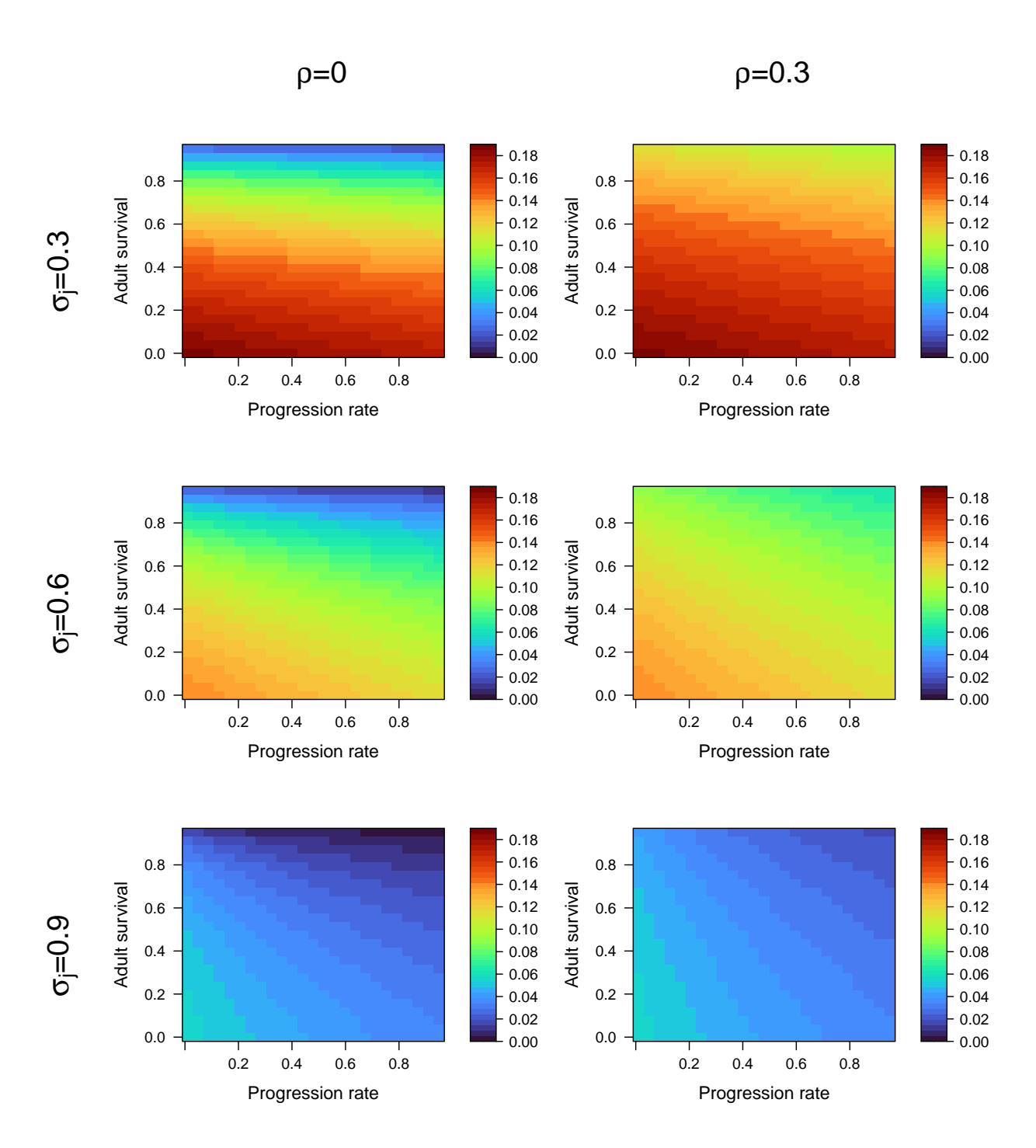


Figure S8: Strength of density effects on compensation when juvenile progression rate is density-dependent. Details are the same as Figure S7.

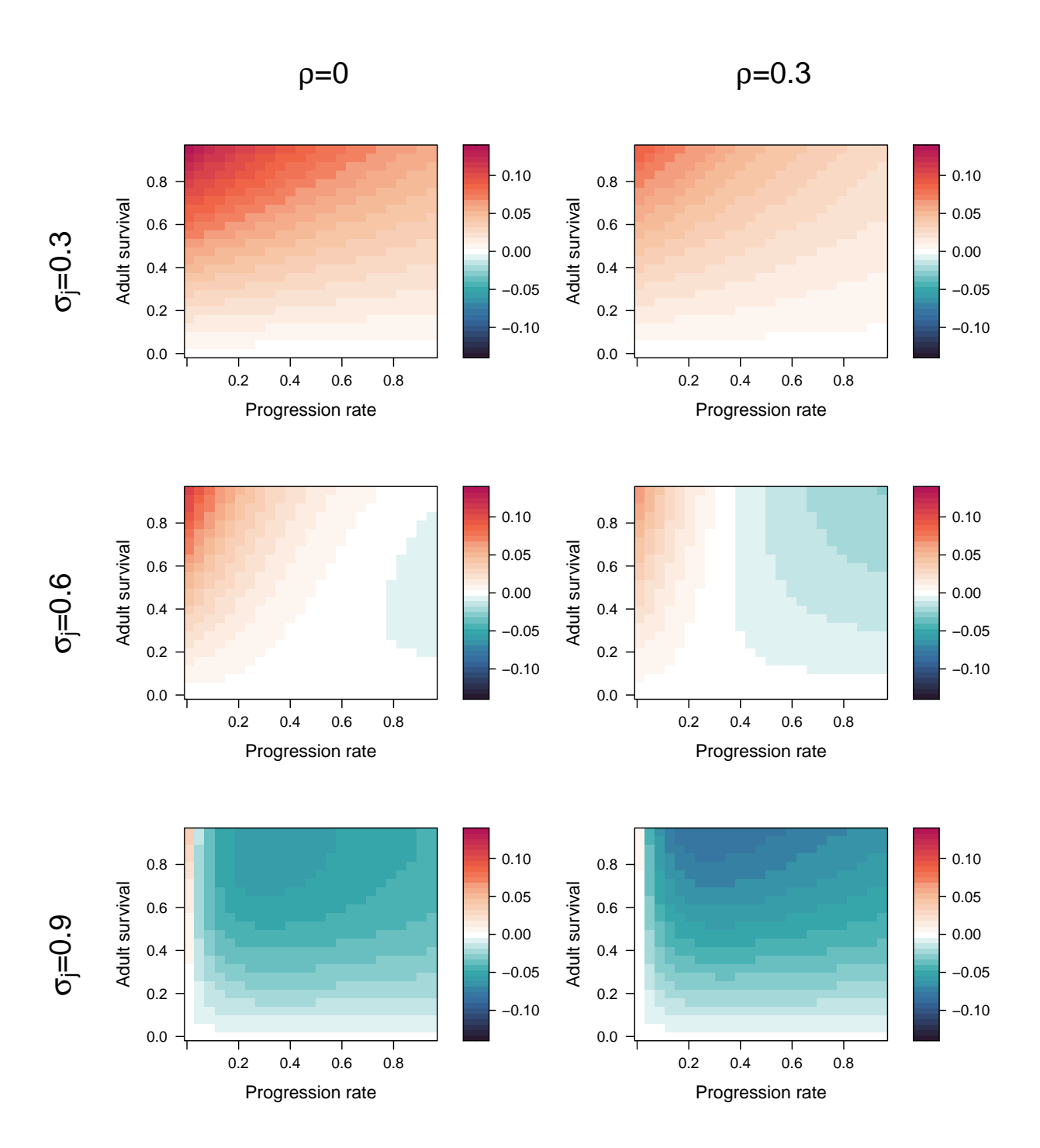


Figure S9: Strength of density effects on compensation when adult survival is density-dependent. Details are the same as Figure S7.

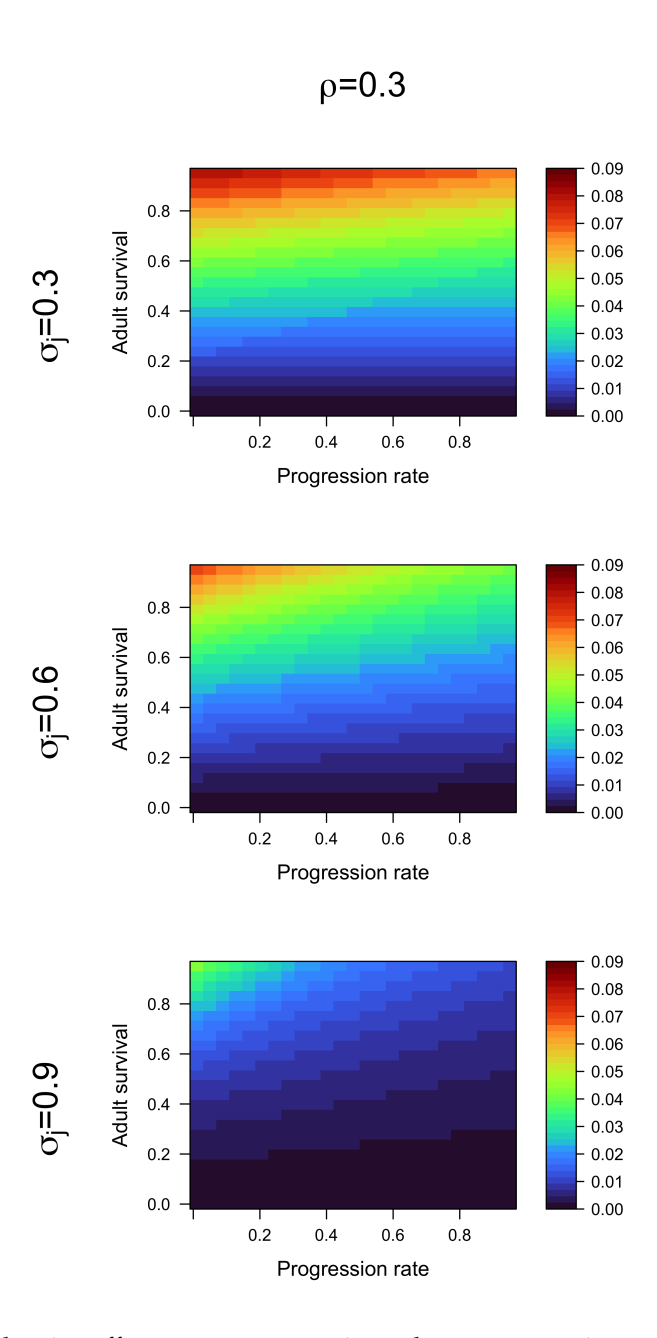


Figure S10: Strength of density effects on compensation when retrogression rate is density-dependent. Details are the same as Figure S7.

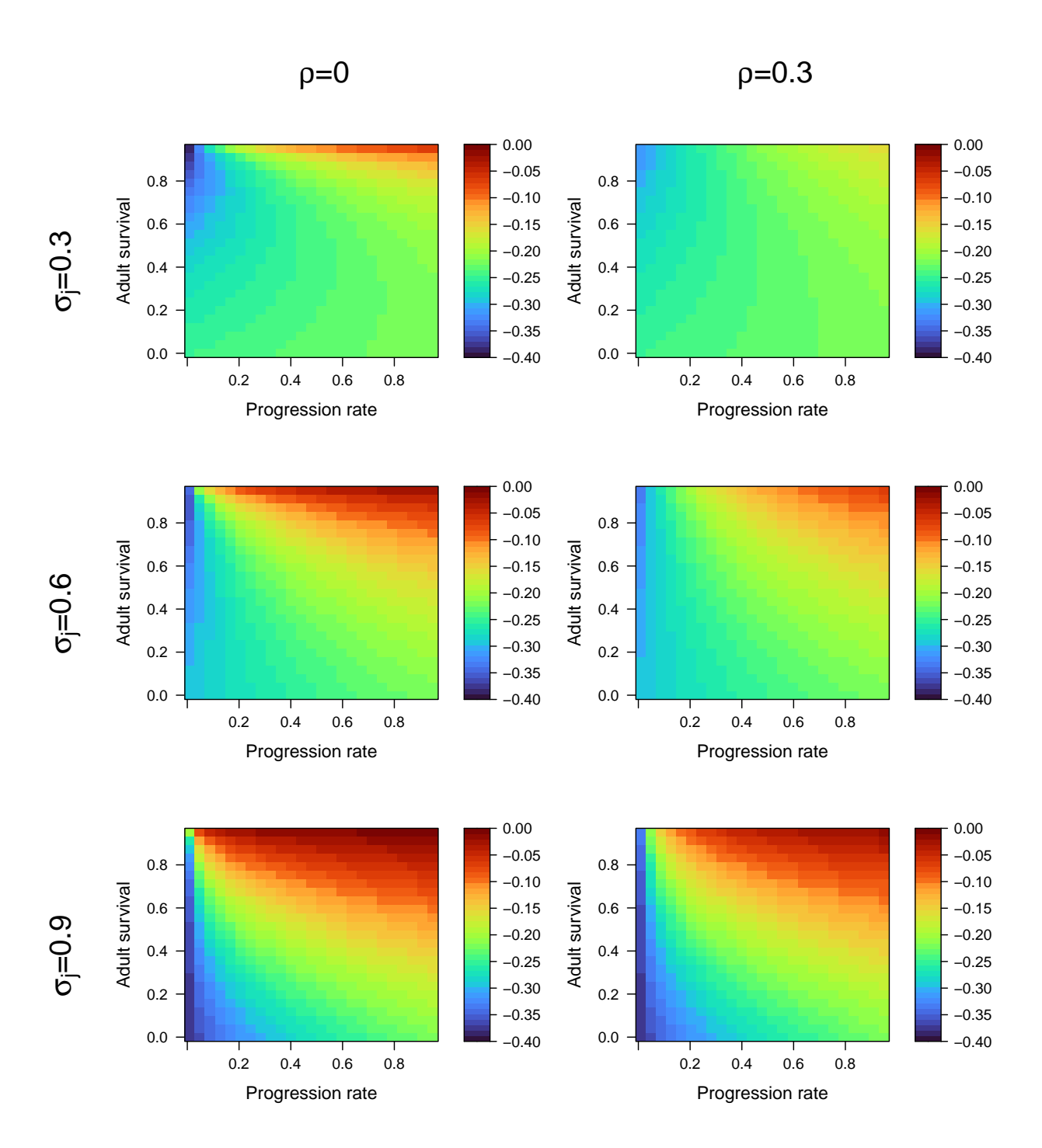


Figure S11: Strength of density effects on compensation when reproductive output is density-dependent. Details are the same as Figure S7.

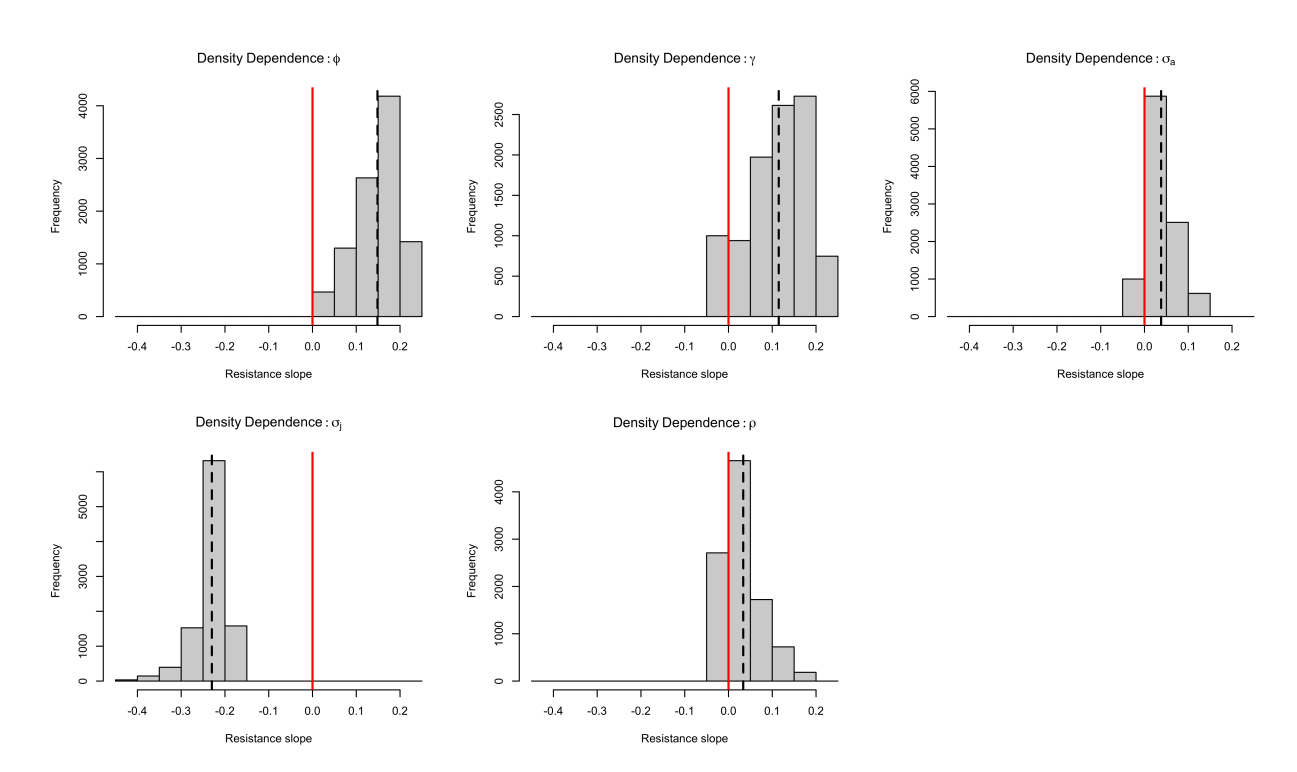


Figure S12: The distribution of resistance slope values depends on which vital rate is the target of density dependence. Details are the same as in Figure S6.

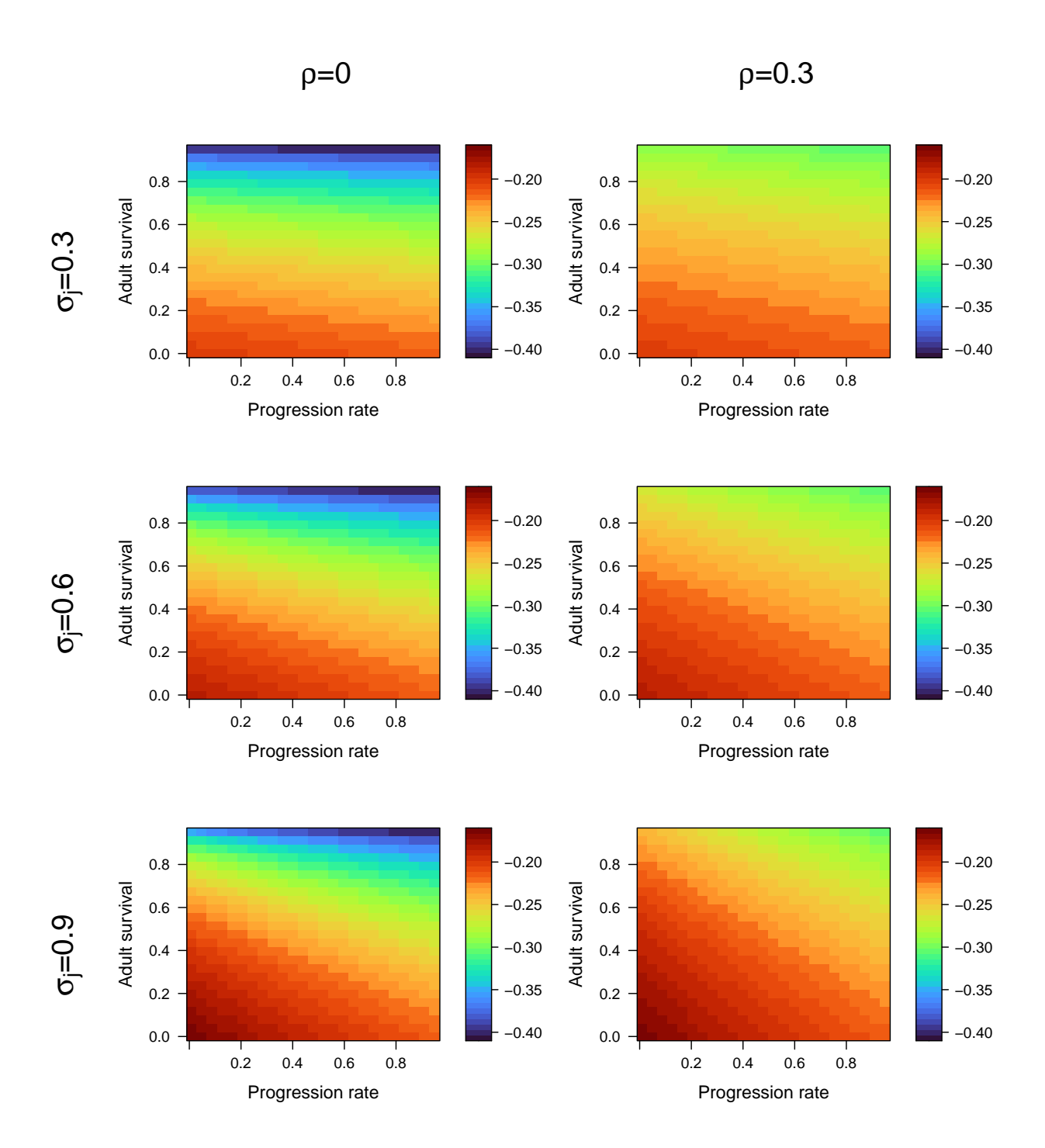


Figure S13: Strength of density effects on resistance when juvenile survival is density-dependent. Details are the same as Figure S7.

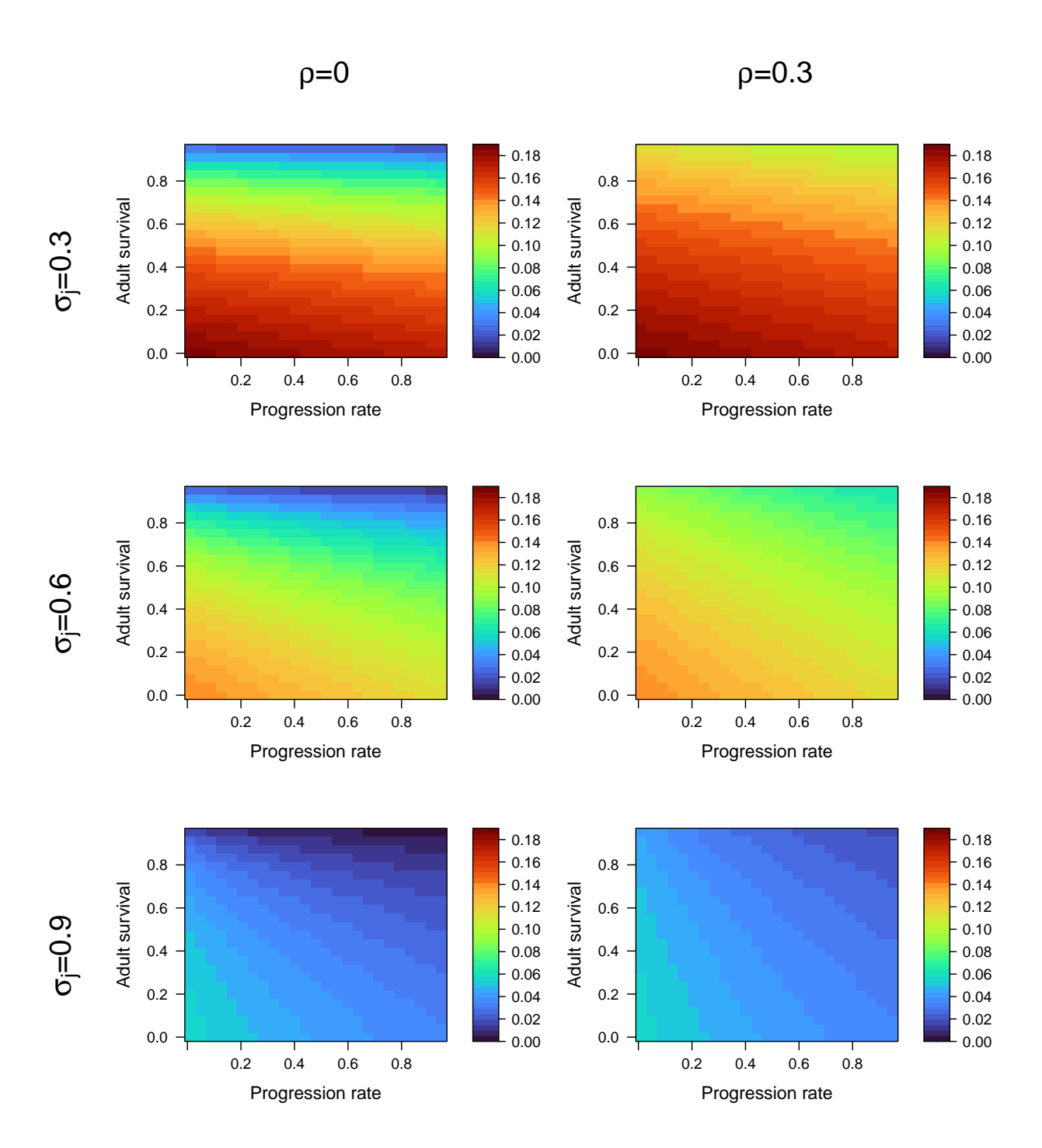


Figure S14: Strength of density effects on resistance when juvenile progression rate is density-dependent. Details are the same as Figure S7.

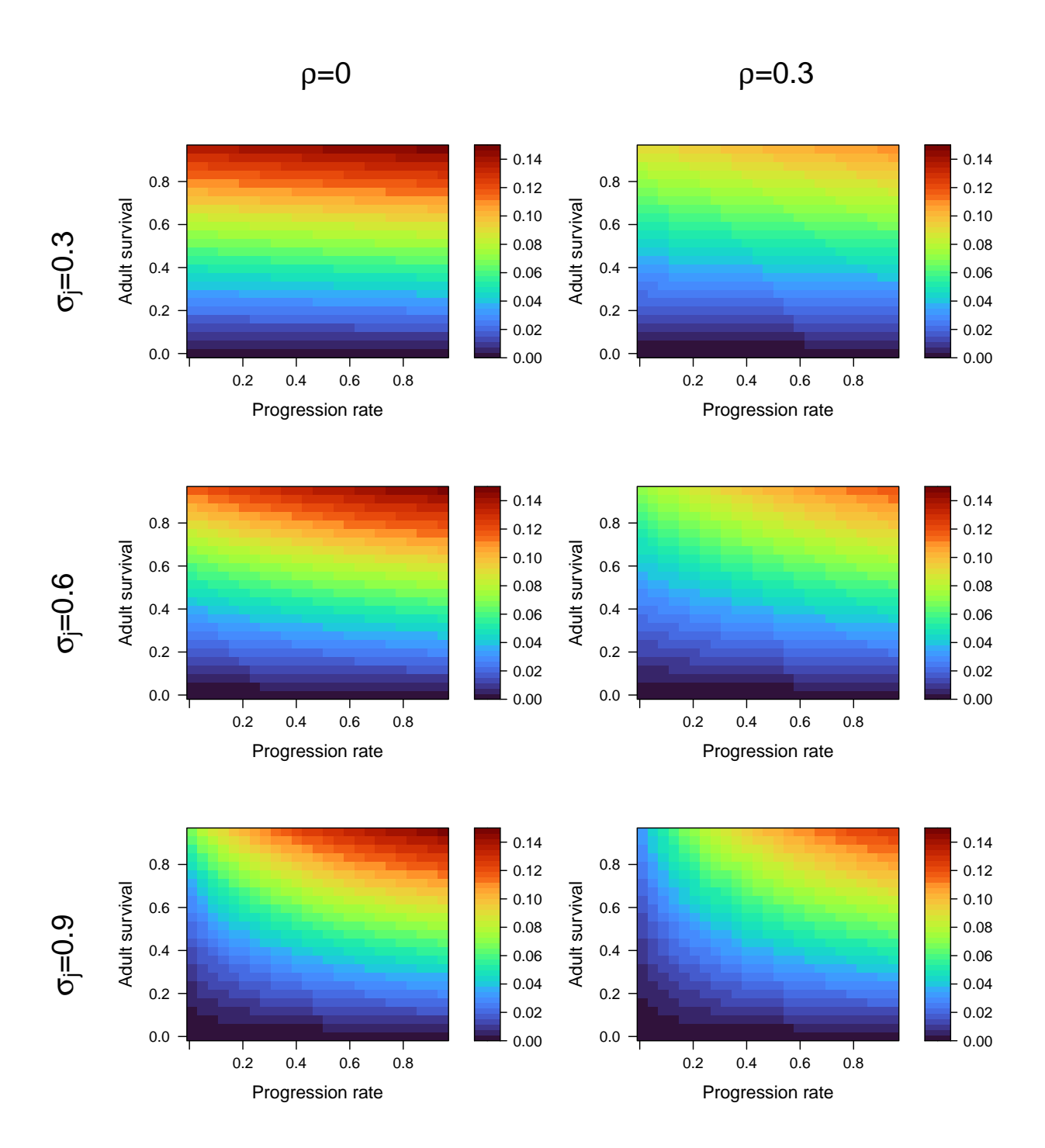


Figure S15: Strength of density effects on resistance when adult survival is density-dependent. Details are the same as Figure S7.

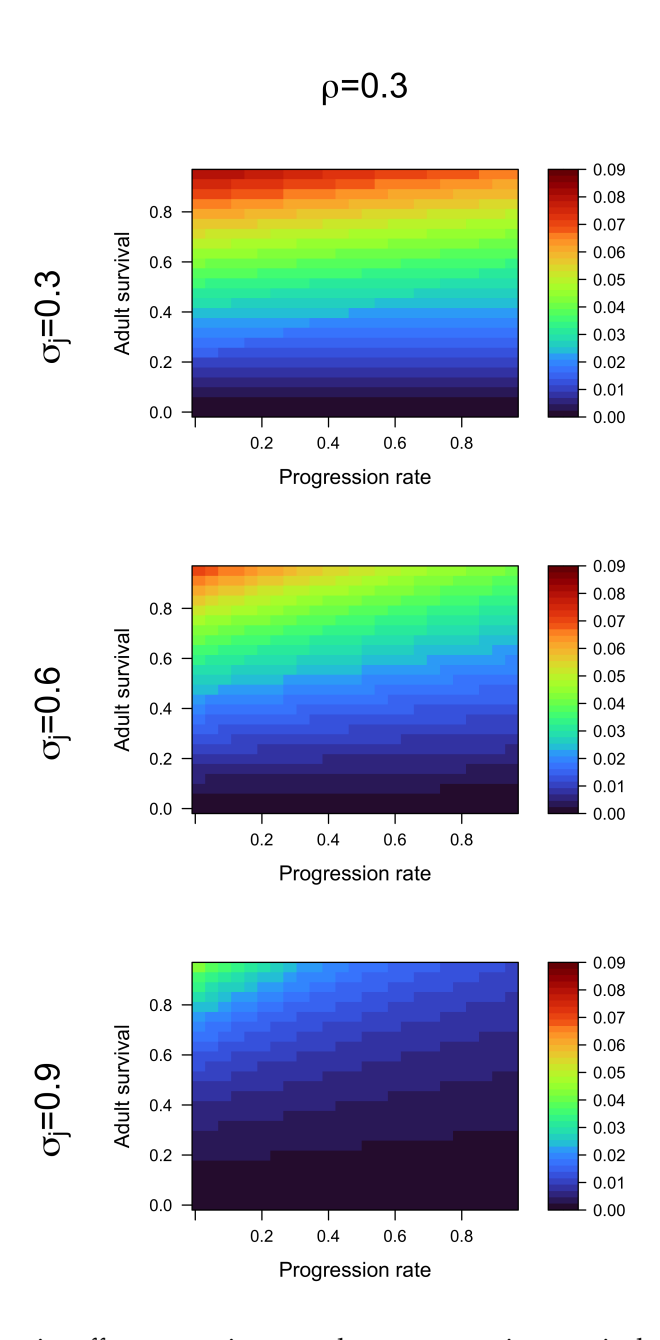


Figure S16: Strength of density effects on resistance when retrogression rate is density-dependent. Details are the same as Figure S7.

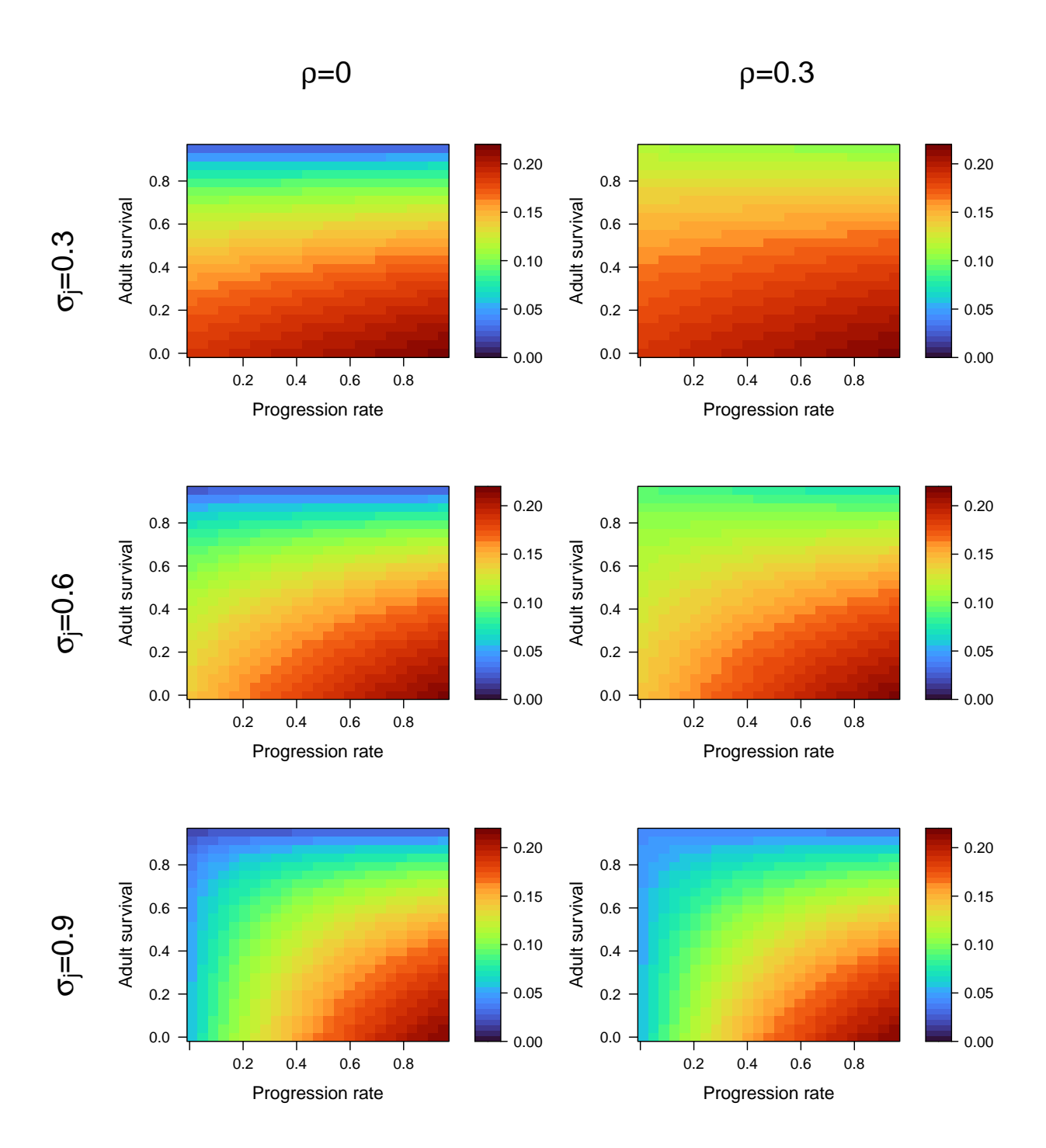


Figure S17: Strength of density effects on resistance when reproductive output is density-dependent. Details are the same as Figure S7.

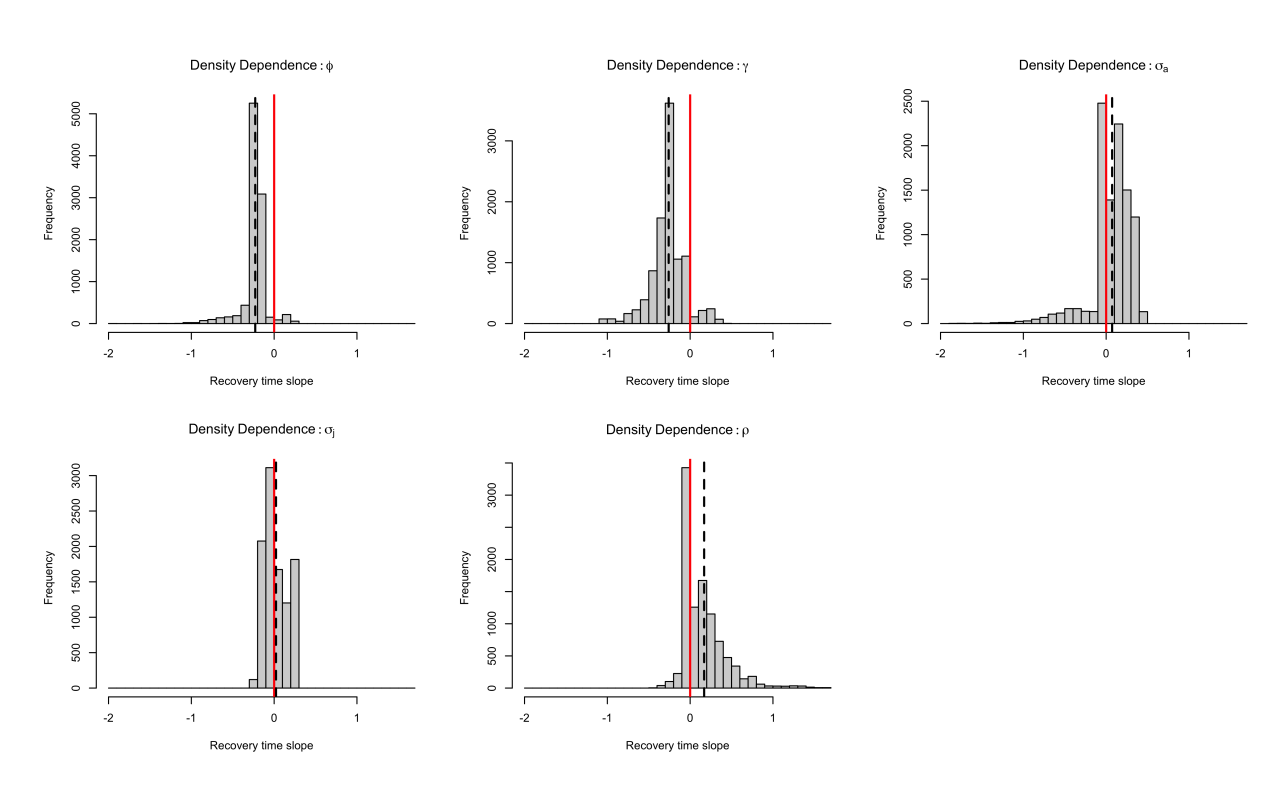


Figure S18: The distribution of density-independent recovery time slope values depends on which vital rate is the target of density dependence. Details are the same as in Figure S6.

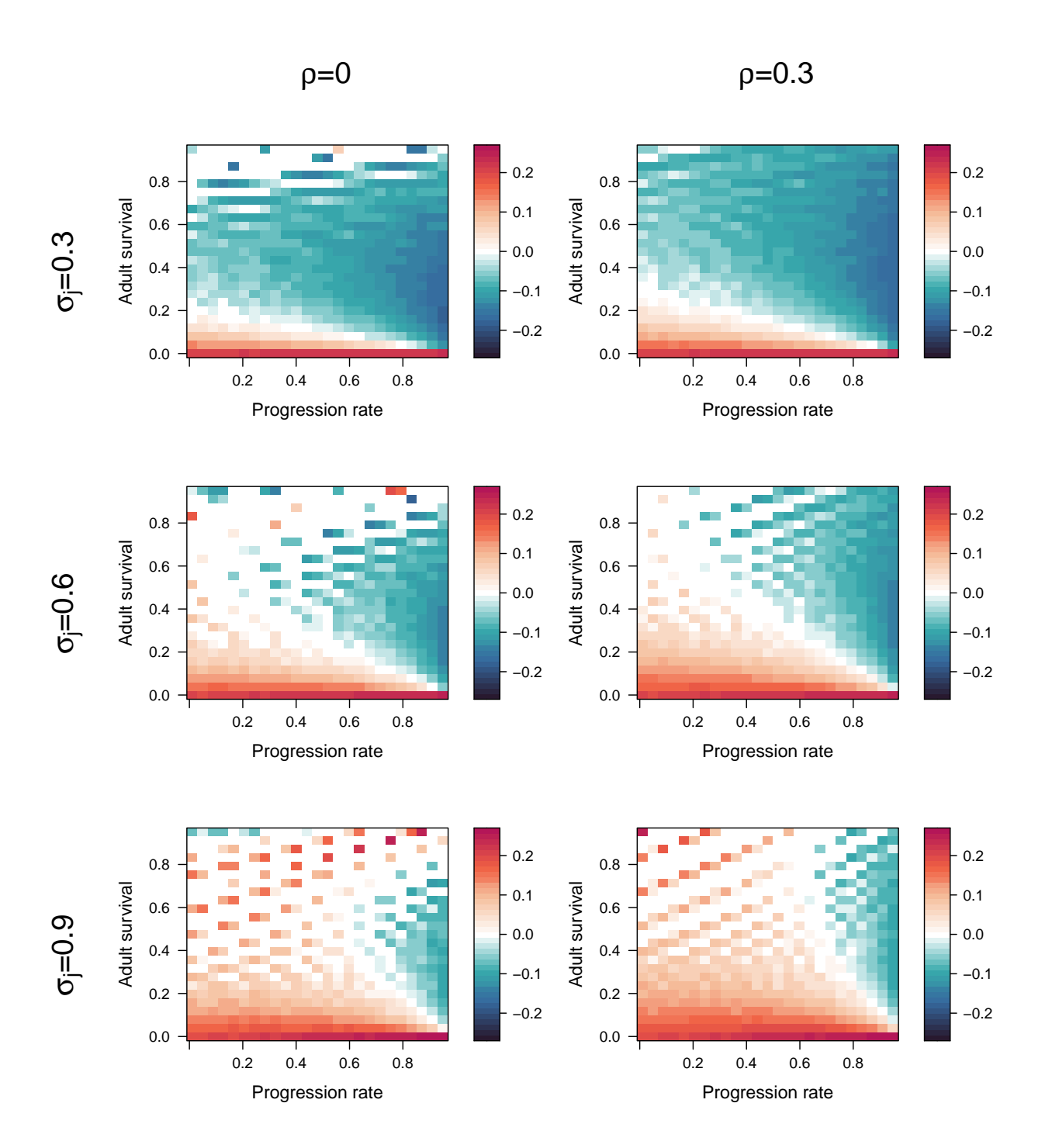


Figure S19: Strength of density effects on density-independent recovery time when juvenile survival is density-dependent. Details are the same as Figure S7.

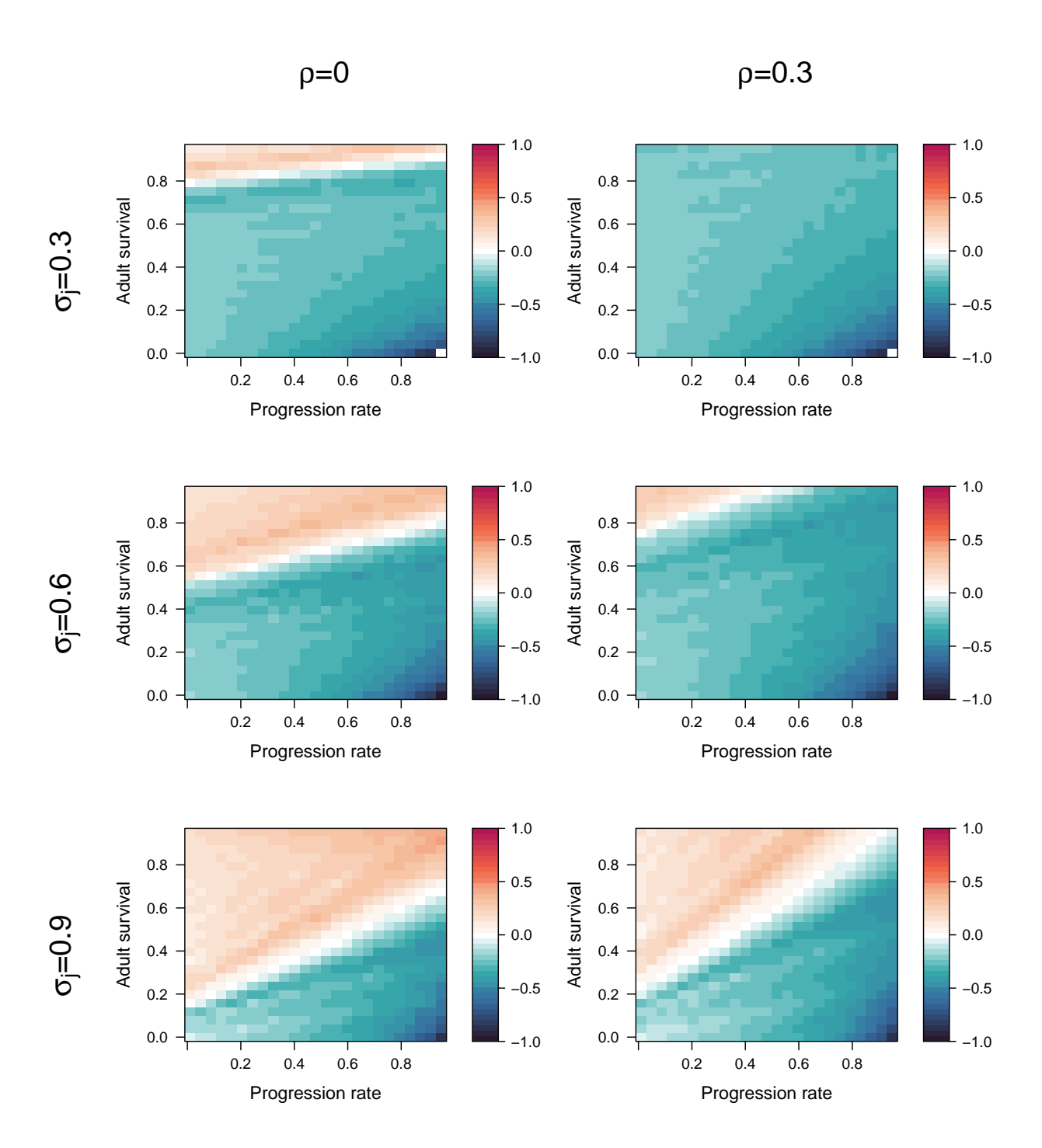


Figure S20: Strength of density effects on density-independent recovery time when juvenile progression rate is density-dependent. Details are the same as Figure S7.

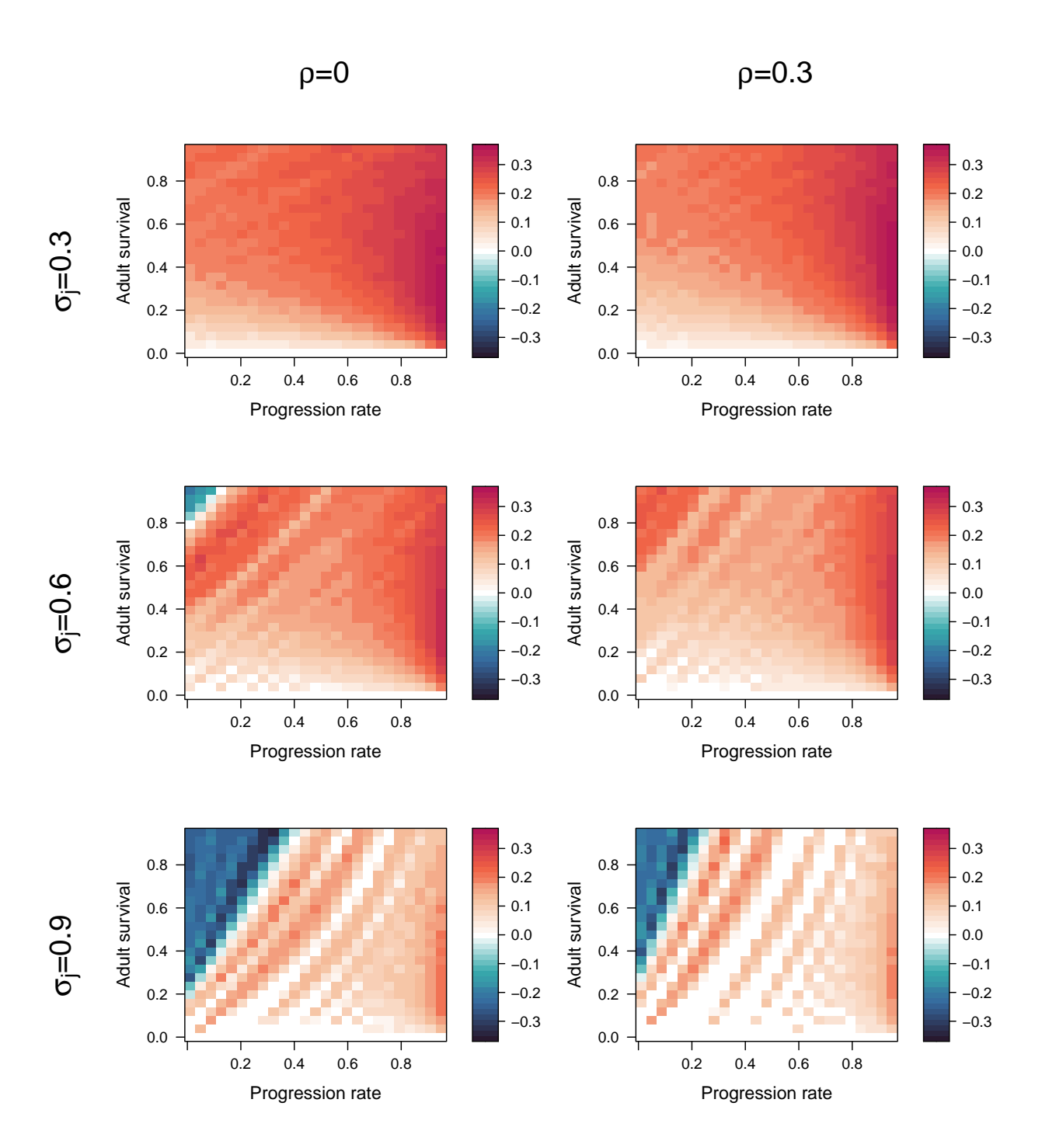


Figure S21: Strength of density effects on density-independent recovery time when adult survival is density-dependent. Details are the same as Figure S7.

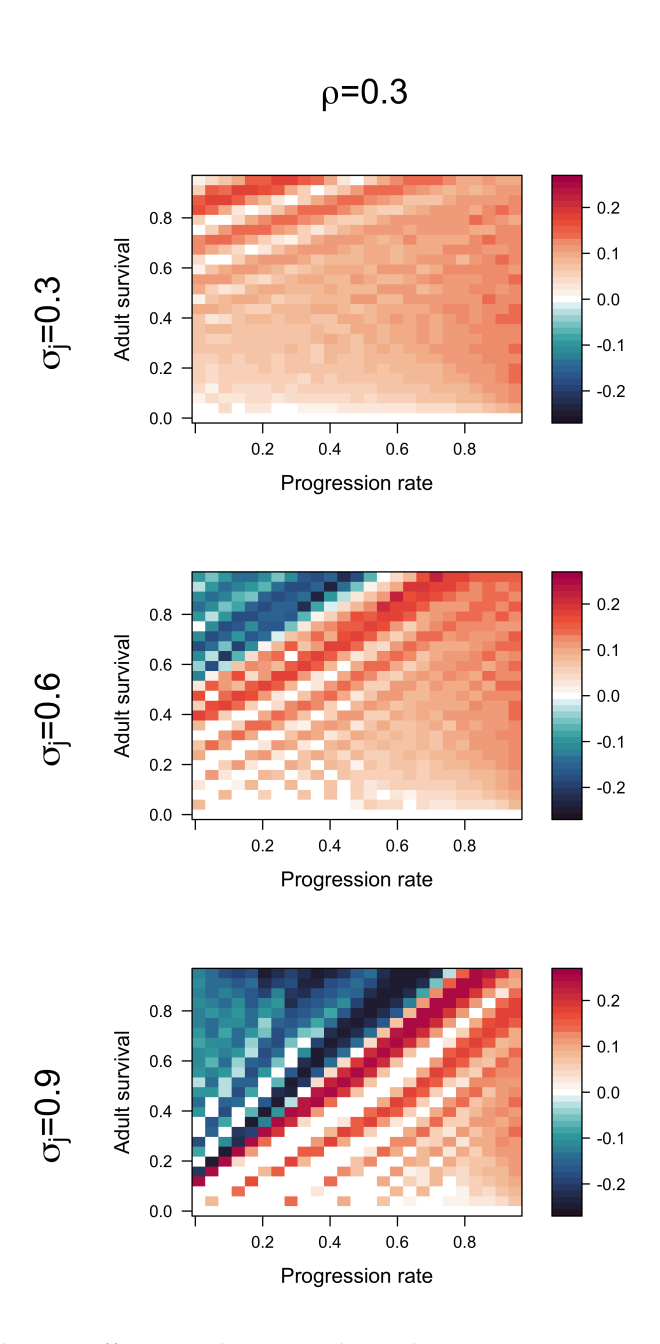


Figure S22: Strength of density effects on density-independent recovery time when retrogression rate is density-dependent. Details are the same as Figure S7.

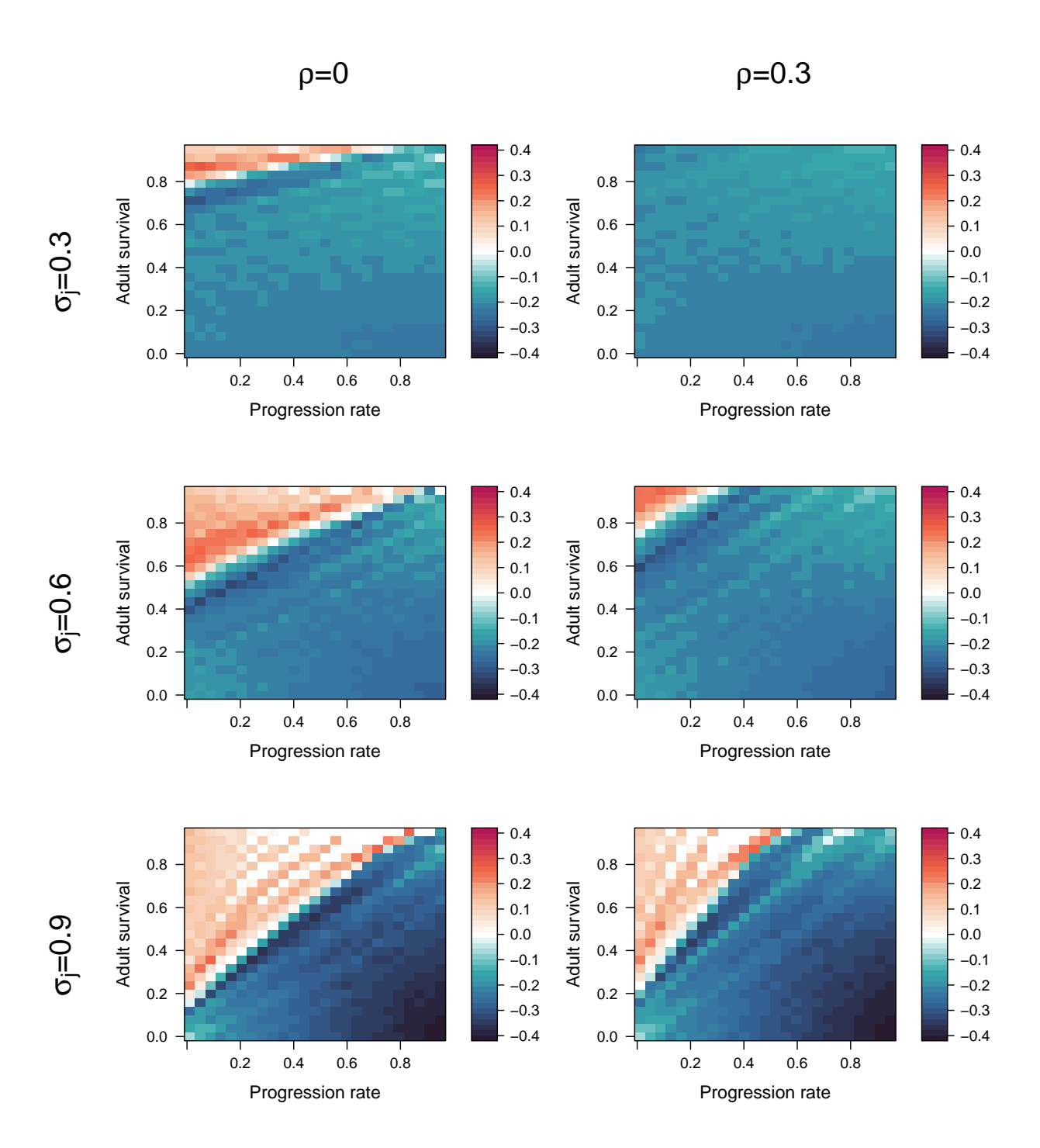


Figure S23: Strength of density effects on density-independent recovery time when reproductive output is density-dependent. Details are the same as Figure S7.

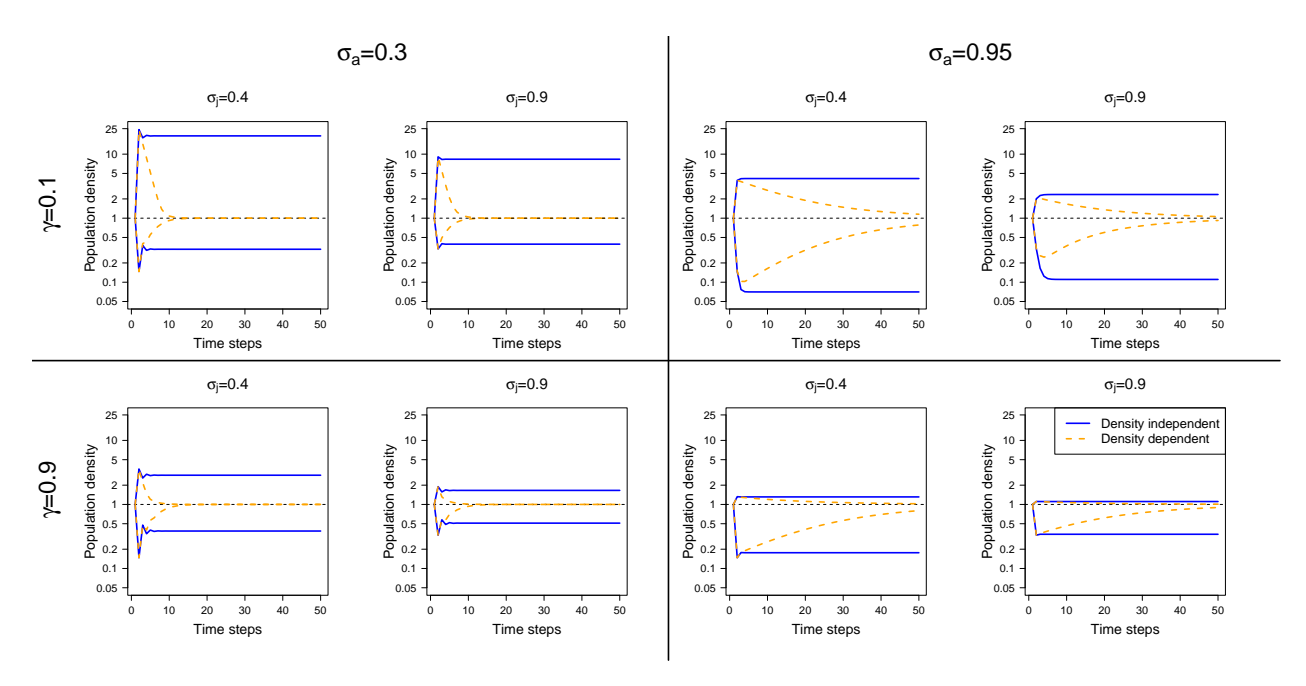


Figure S24: Variation in transient envelope patterns across our set of virtual species and between density-dependent and density-independent models. In this scenario, density dependence operates on juvenile survival (σ_i) .

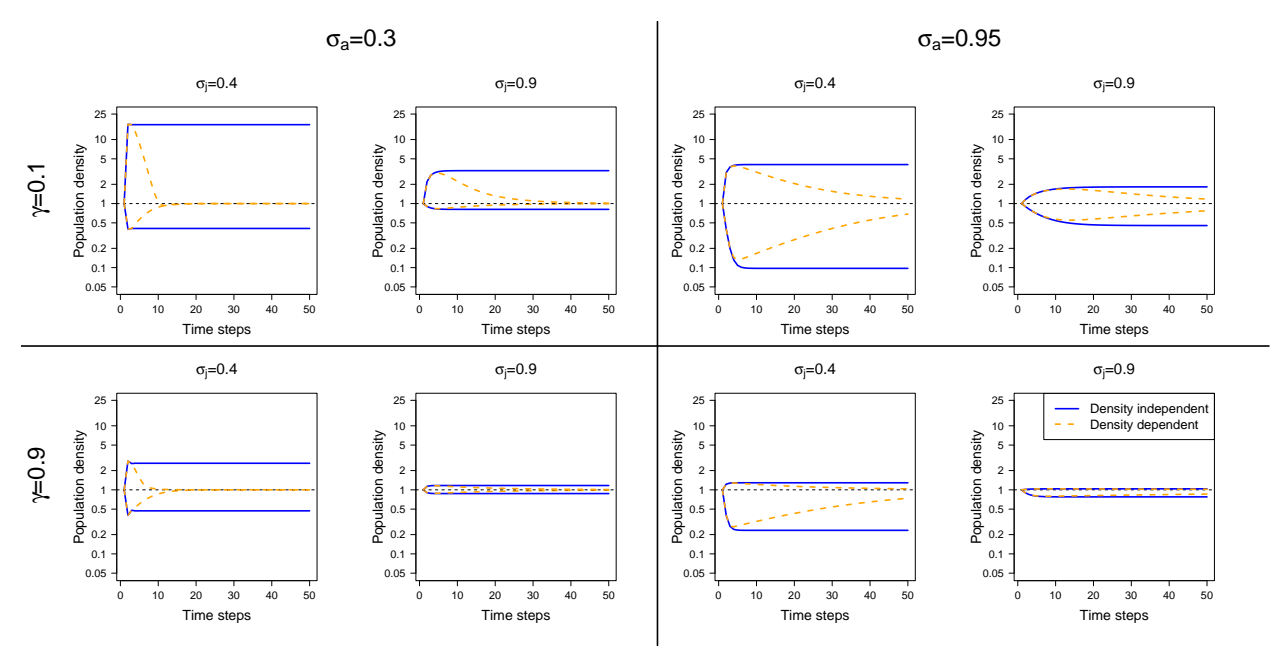


Figure S25: Variation in transient envelope patterns across our set of virtual species and between density-dependent and density-independent models. In this scenario, density dependence operates on progression rate (γ).

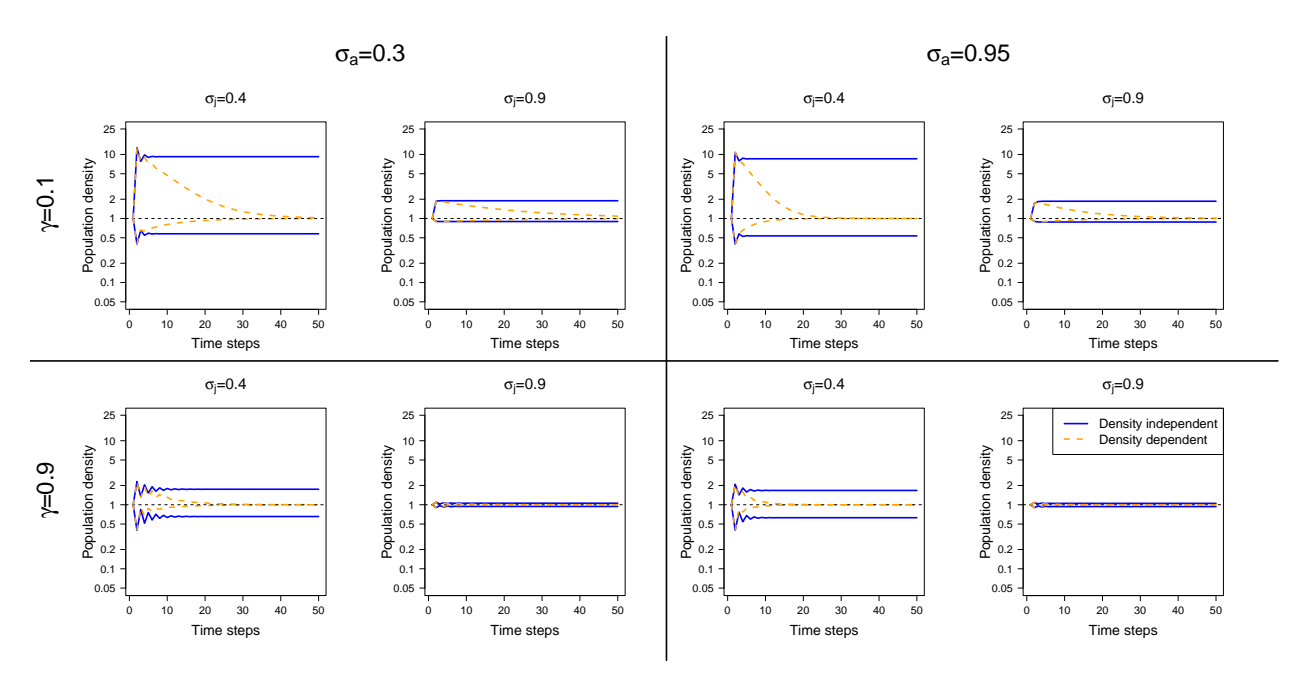


Figure S26: Variation in transient envelope patterns across our set of virtual species and between density-dependent and density-independent models. In this scenario, density dependence operates on adult survival (σ_a).

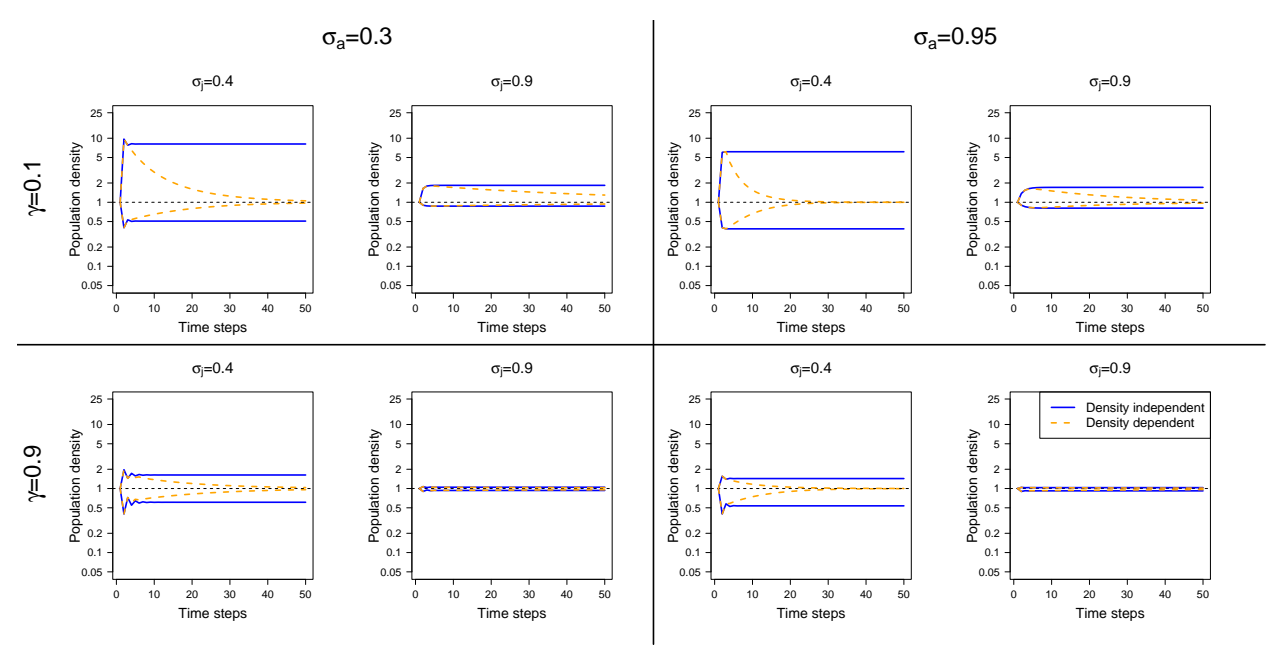


Figure S27: Variation in transient envelope patterns across our set of virtual species and between density-dependent and density-independent models. In this scenario, density dependence operates on retrogression rate (ρ).

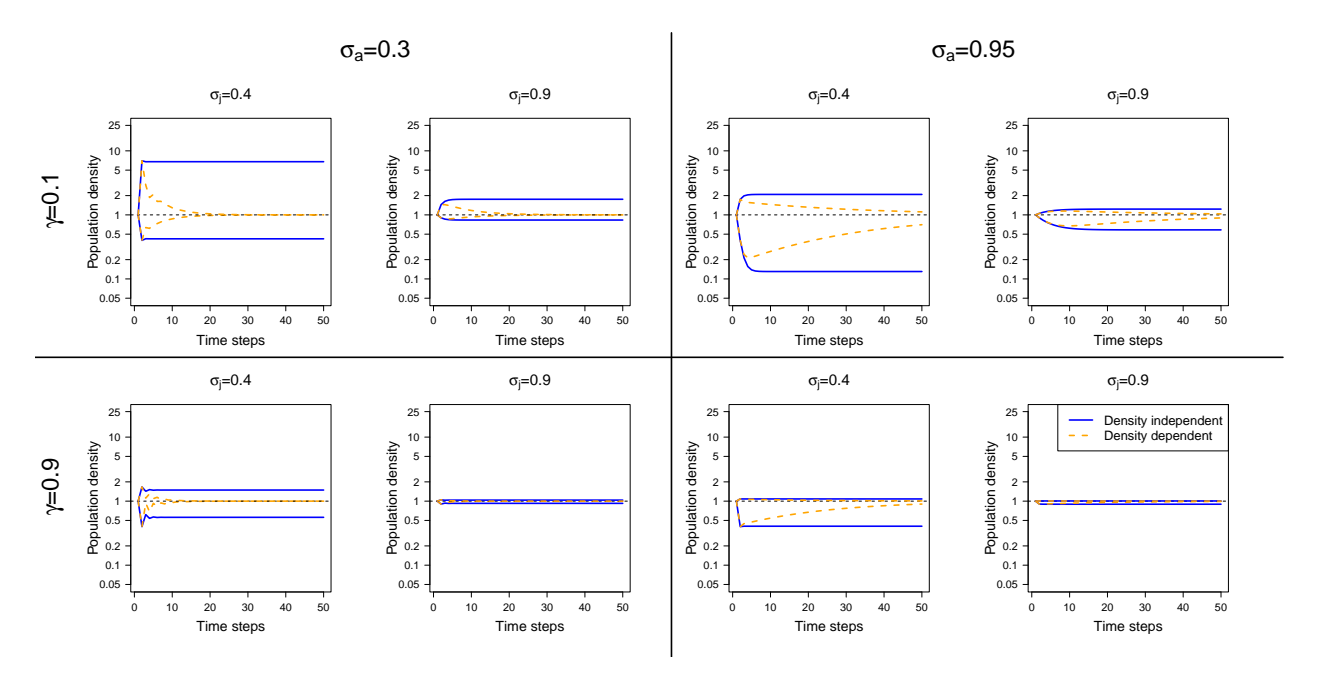


Figure S28: Variation in transient envelope patterns across our set of virtual species and between density-dependent and density-independent models. In this scenario, density dependence operates on reproductive output (ϕ) .

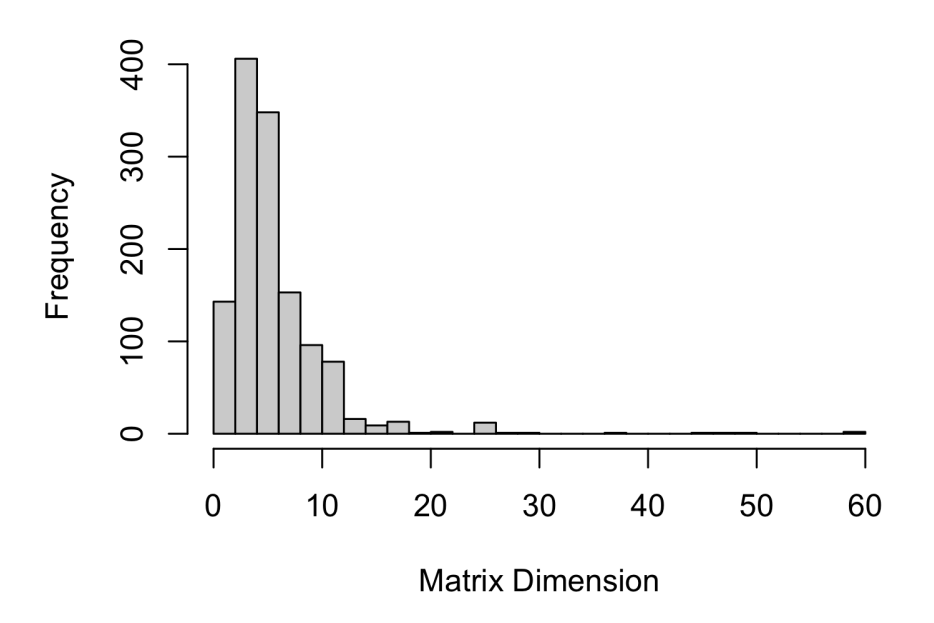


Figure S29: The matrix dimensions for empirical models used in selecting virtual species models. The matrix dimension is the number of classes included in the projection matrix. Before collapsing all the models to 2×2 , most of the models were larger, representing more complex life cycles than represented by our two-stage model (Supplemental Materials Table S4).